ORIGINAL ARTICLE

LXR-dependent regulation of macrophage-specific reverse cholesterol transport is impaired in a model of genetic diabesity

TERESA L. ERRICO[1], KAREN ALEJANDRA MÉNDEZ-LARA[1], DAVID SANTOS, NÚRIA CABRERIZO, LUCÍA BAILA-RUEDA, JARI METSO, ANA CENARRO, EVA PARDINA, ALBERT LECUBE, MATTI JAUHIAINEN, JULIA PEINADO-ONSURBE, JOAN CARLES ESCOLÀ-GIL, FRANCISCO BLANCO-VACA[2], and JOSEP JULVE[2]

BARCELONA, MADRID, AND ZARAGOZA, SPAIN, AND HELSINKI, FINLAND

Diabesity and fatty liver have been associated with low levels of high-density lipoprotein cholesterol, and thus could impair macrophage-specific reverse cholesterol transport (m-RCT). Liver X receptor (LXR) plays a critical role in m-RCT. Abcg5/g8 sterol transporters, which are involved in cholesterol trafficking into bile, as well as other LXR targets, could be compromised in the livers of obese individuals. We aimed to determine m-RCT dynamics in a mouse model of diabesity, the db/db mice. These obese mice displayed a significant retention of macrophage-derived cholesterol in the liver and reduced fecal cholesterol elimination compared with nonobese mice. This was associated with a significant downregulation of the hepatic LXR targets, including *Abcg5/g8*. Pharmacologic induction of LXR promoted the delivery of total tracer output into feces in db/db mice, partly due to increased liver and small intestine *Abcg5/Abcg8* gene expression. Notably, a favorable upregulation of the hepatic levels of *ABCG5/G8* and *NR1H3* was also observed postoperatively in morbidly obese patients, suggesting a similar LXR impairment in these patients. In conclusion, our data show that downregulation of the LXR axis impairs cholesterol transfer from macrophages to feces in db/db mice, whereas the induction of the LXR axis partly restores impaired m-RCT by elevating the liver and small intestine expressions of *Abcg5/g8*. (Translational Research 2017;■:1–17)

[1] These authors contributed equally to this work.

[2] These authors are co-principal and co-corresponding authors of this work.

From the Institut de Recerca de l'Hospital de la Santa Creu i Sant Pau – Institut d'Investigacions Biomèdiques Sant Pau (IIB-Sant Pau), Barcelona, Spain; Departament de Bioquímica i Biologia Molecular, Universitat Autònoma de Barcelona, Barcelona, Spain; CIBER de Diabetes y Enfermedades Metabólicas Asociadas, Madrid, Spain; CIBER de Enfermedades Cardiovasculares, Madrid, Spain; Unidad Clínica y de Investigación en Lípidos y Arteriosclerosis, Hospital Universitario Miguel Servet, Instituto de Investigación Sanitaria Aragón (IIS Aragón), Zaragoza, Spain; National Institute for Health and Welfare, Genomics and Biomarkers unit, and Minerva Foundation Institute for medical Research, Biomedicum, Helsinki, Finland; Departament de Bioquímica i Biomedicina Molecular, Facultat de Biologia, Universitat de Barcelona, Barcelona, Spain; Unitat de Recerca en Diabetes i Metabolisme, Institut de Recerca Hospital Universitari Vall d'Hebron, Barcelona, Spain.

Submitted for publication March 3, 2017; accepted for publication May 11, 2017.

Reprint requests: Dr Francisco Blanco-Vaca or Josep Julve, IIB-Sant Pau, C/Sant Antoni M. Claret 167, 08025 Barcelona, Spain; e-mail: fblancova@santpau.cat, jjulve@santpau.cat.

1931-5244/$ - see front matter

http://dx.doi.org/10.1016/j.trsl.2017.05.004

Abbreviations: ABC = ATP-binding cassette transporters; apo = apolipoprotein; CVD = cardiovascular disease; HDL = high-density lipoprotein; HDL-C = HDL cholesterol; LDL = low-density lipoprotein; LDL-C = LDL cholesterol; m-RCT = in vivo macrophage-specific reverse cholesterol transport; T2D = type 2 diabetes mellitus

AT A GLANCE COMMENTARY

Errico TL, et al.

Background

Diabesity and fatty liver have been associated with decreased HDL cholesterol and thus could impair macrophage-specific reverse cholesterol transport (m-RCT). m-RCT is considered one of the most important anti-atherogenic HDL properties, which could be compromised in obese individuals.

Translational Significance

We present evidence suggesting that LXR signaling is defective in the liver of both obese mouse and patients. In particular, this defective signaling affects two main hepatic sterol transporters, Abcg5/g8, which are involved in hepatobiliary cholesterol trafficking. m-RCT dynamics was partly restored by a potent LXR agonist in the mouse. Notably, a commensurate favorable up-regulation in the hepatic gene expression of both transporters, as well as an improvement in non-alcoholic fatty liver, was also observed in obese patients subjected to bariatric surgery. This evidences the potential of targeting LXR signaling as a strategy to improve m-RCT in diabesity.

INTRODUCTION

Obesity is a major health burden in Westernized societies and leads to several cardiometabolic complications, including insulin resistance, hepatic steatosis, and abnormal plasma lipid levels, including decreased high-density lipoprotein (HDL) cholesterol (HDL-C).[1,2] The efflux capacity of HDL-C has been demonstrated to be a better indicator of cardiovascular risk than HDL-C.[3] This HDL property is considered the first step in the in vivo macrophage-specific reverse cholesterol transport (m-RCT),[4] whereby excess cholesterol is removed via HDL from macrophages to the liver for fecal excretion. This key physiological process comprises various regulatory steps in different body compartments and is considered to be atheroprotective. Given that there are no suitable assays for the evaluation of the rate of m-RCT in humans, the factors that modulate the efficiency of this pathway have been extensively studied in mice.

m-RCT may be altered in several metabolic diseases, including obesity and T2D.[5-7] In support of this hypothesis, m-RCT has been found to be impaired in a mouse model of obesity (ie, db/db mice) due to defects in the leptin axis.[8] Consistently, db/db mice also show decreased biliary cholesterol elimination,[9] and this metabolic phenotype is frequently associated with lower hepatic levels of 2 ABC cholesterol transporters (ie, Abcg5 and Abcg8). Insomuch as these 2 transporters are involved in the hepatobiliary transport of cholesterol in both mice[10-16] and humans,[17,18] a reduction in their hepatic abundance would compromise hepatobiliary cholesterol trafficking and, hence, m-RCT. Abcg5 and Abcg8, which are primarily regulated at the transcriptional level, are also well-recognized liver X receptor (LXR) gene targets.[13,19,20] However, recent findings indicate that post-transcriptional mechanisms reduce liver Abcg5/g8 protein abundance in mice with defective leptin signaling.[9] In this study, we tested the hypothesis that the impairment of m-RCT in db/db mice would be directly related to the hepatic and intestinal abundance of Abcg5/g8 partly due to an impaired LXR signaling.

MATERIALS AND METHODS

Mice. All animal procedures were reviewed and approved by the Institutional Animal Care Committee and Use Committee of the Institut de Recerca de l'Hospital de la Santa Creu i Sant Pau, and the methods were carried out in accordance with the approved guidelines. Obese male 14- to 16-week-old db/db mice on a C57BL/6J genetic background were obtained from Jackson Laboratories (Bar Harbor, Maine; #000674). During the administration of the LXR agonist, male db/db mice were matched for body weight and randomized into 2 groups (ie, control [Ctrl]-LXR and db/db-LXR) that were treated with daily intragastric doses of T0901317 (20 mg/kg; Alexis Biochemicals) or a vehicle solution (1.0% wt./vol. carboxymethylcellulose medium viscosity; ie, Ctrl and db/db) for 10 days. All mice were maintained on a regular chow diet (Safe, Scientific Animal Food & Engineering). All animals were kept in a temperature-controlled environment (20°C) with a 12-hour (h) light/dark cycle. Food and water were provided ad libitum.

Genotyping was performed as indicated on the Jackson laboratory website (http://jaxmice.jax.org). At the end of the studies, mice were euthanized and exsanguinated by cardiac puncture. Blood was collected, and serum was obtained by centrifugation. Food intake was monitored for 2 days before the animals were euthanized.

Human subjects. A total of 10 morbidly obese patients who were scheduled to undergo Roux-en-Y gastric bypass surgery and liver biopsy at baseline and 12 months after intervention were evaluated. All procedures were performed in accordance with the ethical standards of the institutional and/or national research committee and with the 1964 Declaration of Helsinki and its later amendments or comparable ethical standards. The study protocol was reviewed and accepted by the ethics committee of the Hospital de la Vall d'Hebron in Barcelona. Informed consent was obtained from all participants included in the study. The subjects presented the necessary indications for bariatric surgery: BMI >40 kg/m^2 or greater than 35 kg/m^2 with at least one comorbidity, including hypertension, type 2 diabetes (T2D), dyslipidemia, obstructive sleep apnea, or weight-induced rheumatological disease. The diagnostic criteria used for T2D, hypertension, and metabolic syndrome are detailed in the National Cholesterol Education Program.[21] In the present study, 3 of 10 obese subjects included in the study presented with T2D (30%). All subjects were free of inflammatory and infectious diseases, and none of the subjects were receiving anti-obesity or anti-inflammatory drugs at the time of the study. Patients were excluded if they had neoplastic, renal, or active systemic diseases, hypothyroidism, or an endocrine disease other than diabetes. All patients reported that their weight had been stable for the previous 3 months. None of the diabetic patients were being treated with insulin. Blood samples and liver specimens were obtained from each subject at the time of gastric bypass surgery and 12 months after gastric bypass surgery. Body weight, height, and waist and hip circumferences were measured according to standardized procedures.[22] The amount of total fat was calculated as previously described.[23]

Biochemical analyses. Plasma lipid analyses were performed enzymatically with commercial kits adapted to a COBAS c501 autoanalyzer (Roche Diagnostics). Free cholesterol and phospholipids were evaluated with reagents from Wako Diagnostics. HDL-C was measured in apoB-depleted plasma obtained after precipitation with phosphotungstic acid and magnesium ions (Roche Diagnostics). In the human study, the lipid profile included total cholesterol (Roche Diagnostics), triglycerides (Roche Diagnostics), LDL cholesterol (LDL-C; LDL-C Plus, Roche Diagnostics), and HDL-C (HDL-C Plus, Roche Diagnostics). Mouse apoA-I expression was determined with an ELISA kit, and the wells were coated with a polyclonal rabbit antibody against mouse apoA-I as previously reported.[24] The concentration of 27-hydroxycholesterol in plasma and liver was measured via high-performance chromatography tandem mass spectrometry (HPLC-MS/MS) after lipid extraction, as described previously.[25]

Lipoprotein fractions were isolated from pooled plasma samples by sequential ultracentrifugation at 100,000 *g* for 24 hours using an analytical fixed-angle rotor (50.3, Beckman Coulter) in all groups of mice. HDL was isolated from either wild-type mice or db/db mice at a density range of between 1.063 and 1.21 g/mL. The lipoprotein subfraction composition was analyzed for lipids, including total cholesterol, free cholesterol, phospholipids and triglycerides, and proteins (total protein content) at the indicated times with the above-mentioned commercial methods. The protein levels in isolated lipoprotein fractions were determined with the bicinchoninic acid assay reagent (Thermoscientific). The composition of HDL, including total and free cholesterol, phospholipids and protein content, was determined in plasma-isolated lipoproteins and was used to calculate the total HDL mass. Lecithin:cholesterol acyltransferase (LCAT) activity toward endogenous lipoproteins labeled with radioactive cholesterol was measured, as previously reported.[26] Phospholipid transfer protein radiometric assay was carried out as previously described.[27]

Quantification of preβ-HDL in mouse plasma. The amount of preβ-HDL formed of preincubation of plasma in the presence of an LCAT inhibitor (1-mM iodoacetate) was quantified by 2-dimensional crossed immunoelectrophoresis, as previously reported.[27] Briefly, freshly isolated plasma samples from mice were either frozen (−80°C) or incubated at 37°C in the presence of iodoacetate to measure the formation of preβ-HDL in vitro. The crossed immunoelectrophoresis consisted of agarose electrophoresis in the first dimension for separation of lipoproteins with their pre-β, β, and α mobilities. Electrophoresis in the second dimension (ie, antigen migration from the first gel into an anti-apoA-I–containing gel) was used to quantitatively precipitate apoA-I. The gel was stained with Coomassie brilliant blue R250 and subsequently dried. Areas under the preβ-HDL and α-HDL peaks were calculated. The preβ-HDL area is expressed as a percentage of the sum of α-HDL and preβ-HDL areas.

Fecal and liver cholesterol analyses. Stools from individually housed mice fed ad libitum and with free access to water were collected over 2 days. Mice were euthanized and exsanguinated by cardiac puncture at the end of the study, and livers were removed after being perfused extensively with saline. In the human study, liver lipids were extracted from a 100-mg piece of liver with isopropyl alcohol-hexane (2:3; v:v). After the addition of Na_2SO_4, the hexane phase was isolated, dried with nitrogen, reconstituted with 0.5% sodium cholate, and sonicated for 10 minutes (50 Hz) before lipid measurements.

HDL kinetics. Autologous [^{3}H]-cholesteryl oleate-labeled HDL ([^{3}H]-HDL; containing $5 \cdot 10^5$ cpm; 7500 cpm/nmol; 75 nmol injected per mouse) obtained from db/db mice and Ctrl littermates was isolated and injected intravenously into each mouse as previously described.[28] Serum was collected into tubes at 1, 2, 6, 24, and 48 hours under isofluorane anesthesia. Serum decay curves for the [^{3}H]-tracer were normalized to radioactivity at the initial 2-minute time point after tracer injection. Fractional catabolic rates were calculated from the area under the serum disappearance curves fitted to a nonlinear, 2-phase exponential decay model. At the end of the experiment, livers and feces were collected and subjected to lipid extraction. Liver and fecal [^{3}H]-tracer concentrations, expressed as % of injected dose, were also determined.

Metabolic fate of orally gavaged cholesterol. In independent experiments, mice were orally gavaged with 3 μCi of [^{14}C]-cholesterol per mouse (PerkinElmer) in an intragastric load of 150 μL of olive oil (Carbonell, 79% oleic acid) as a vehicle. Subsequently, blood samples (50 μL) were taken at the times indicated. At the end of the experiment, livers and feces were collected and subjected to lipid extraction. Liver [^{3}H]-tracer concentration, expressed as % of administered dose, was also determined.

Measurement of m-RCT in vivo. [^{3}H]-Cholesterol-labeled J774 macrophages were prepared and intraperitoneally injected into mice as described previously.[29] Mice were then individually housed in metabolic cages and stools were collected over the next 2 days. Plasma radioactivity was determined at 48 hours by liquid scintillation counting. HDL-associated [^{3}H]-cholesterol was measured after precipitation of apoB-containing lipoproteins with phosphotungstic reagent. At that point, mice were euthanized and livers were collected. Liver and fecal lipids were extracted with isopropyl alcohol or hexane. The lipid layer was collected and evaporated, and [^{3}H]-cholesterol radioactivity was measured by liquid scintillation counting. The distribution of [^{3}H]-cholesterol between free cholesterol and cholesteryl ester was determined via thin-layer chromatography. The [^{3}H]-tracer detected in fecal biliary acids was determined in the remaining aqueous phase of fecal material extracts. The amount of [^{3}H]-tracer was either expressed as a fraction of the injected dose or relative to Ctrl, which was taken as 100%. During the pharmacologic activation of LXR in mice, [^{3}H]-cholesterol-labeled J774 macrophages were injected on day 8 and animals were euthanized on day 10 of LXR agonist administration.

Evaluation of macrophage-specific cholesterol efflux to plasma HDL ex vivo. Ex vivo cholesterol efflux was determined using J774 [^{3}H]-cholesterol-labeled mouse macrophages by adapting the previously described methodology.[29] Aliquots of plasma HDL were used as acceptors in cholesterol efflux experiments. Briefly, cellular cholesterol was labeled for 48 hours with 2 μCi/well [1α, 2α(n)-^{3}H]-cholesterol (GE Healthcare Europe GmbH, Germany). The labeled cells were equilibrated overnight in 0.2% bovine serum albumin in the presence/absence of 0.3 mM of cyclic adenosine monophosphate (Sigma-Aldrich; to upregulate the expression of *Abca1*) and then incubated for 4 hours at 37°C with 5% apoB-containing lipoprotein-depleted plasmas. The media and cell lysates were collected and analyzed for [^{3}H]-radioactivity by liquid scintillation. Cholesterol efflux (%) was calculated as $cpm_{medium}/(cpm_{cells} + cpm_{medium}) \times 100$. The difference in cholesterol efflux from cells stimulated in the absence and presence of cyclic adenosine monophosphate was defined as Abca1-dependent efflux and represents cholesterol efflux predominantly driven to small, preβ-HDL. Abca1-independent efflux was derived from untreated cells and represents cholesterol efflux predominantly driven to large HDL.

Hepatic levels of Abcg5/g8 protein. Western blot analysis for mouse Abcg5/g8 was performed on homogenized pieces of liver. These were homogenized on ice in 20-mM Tris-HCl buffer (pH 7.5) with proteinase inhibitors (10 μg/mL leupeptin, 20-μg/mL aprotinin, 5-μg/mL pepstatin A, 0.2-mM phenylmethylsulfonylfluoride, and 5-mM ethylenediamine tetraacetic acid) and centrifuged at 700 g for 10 minutes to remove debris. Protein extracts underwent 7.5% SDS-polyacrylamide gel electrophoresis under reducing conditions (25 μg of protein per lane) and were then blotted to nitrocellulose membranes. Immunoreactivity was assessed via specific polyclonal antibodies to mouse Abcg5/g8 (rabbit IgG fraction, 1:5000 dilution; Novus Biologicals) and a goat anti-rabbit HRP-conjugated secondary antibody (1:15,000 dilution; Sigma) and visualized with enhanced

chemiluminescence detection (Thermoscientific). Autoradiograms were scanned and analyzed with the Gel Doc 2000 image analysis program (Bio-Rad). β-Tubulin was used as a load normalizer.

Quantitative real-time RT-PCR analyses. The RNA from both liver and small intestine was isolated via TRIzol reagent (Invitrogen) following the manufacturer's protocol and was purified with the RNeasy Plus Mini Kit (Qiagen). The integrities of the total RNA samples were determined with a bioanalyser. Total RNA was reverse-transcribed with random primers using Oligo $(dT)_{23}$ and a mixture of dNTPs (Sigma), and M-ML reverse transcriptase, RNase H Minus, and Point Mutant (Promega) to generate cDNA. cDNA was subjected to real-time PCR amplification using Taqman Master Mix (Applied Biosystems). Specific mouse Taqman probes (Applied Biosystems) were used for *Abcb11* (Mm00445168_m1), *Abca1* (Mm00442646_m1), *Abcg1* (Mm00437390_m1), *Abcg5* (Mm00446241_m1), *Abcg8* (Mm00445970_m1), *Acaca* (Mm01304257_m1), *Ap-oa1* (Mm00437569_m1), *Cd36* (Mm01135198_m1), *Cyp27a1* (Mm00470430_m1), *Cyp7b1* (Mm00484157_m1), *Fasn* (Mm01253292_m1), *Nr1h3* (Mm00443451_m1), *Pparg* (Mm01184322_m1), *Scarb1* (Mm00450236_m1), *Npc1l1* (Mm01191972_m1) and *Gapdh* (Mm99999915_g1) (reference gene) in mouse tissue gene expression analysis; specific human Taqman probes (Applied Biosystems) were used for *NR1H3* (Hs00172885_m1), *NR1H2* (Hs01027215_g1), *ABCA1* (Hs01059118_m1), *ABCG1* (Hs00245154_m1), *ABCG5* (Hs00223686_m1), *ABCG8* (Hs00223690_m1), and ACTB (Hs99999903_m1; reference gene) in human tissue gene expression analysis. Real-time PCR assays were performed on a C1000 Thermal Cycler coupled to a CFX96 Real-Time System (Bio-Rad Laboratories SA, Life Science Group). All analyses were performed in duplicate. The relative mRNA expression levels were calculated via the $\Delta\Delta$Ct method.

Statistical methods. The data are presented as the mean ± standard error (SE), unless stated otherwise. Statistical analyses were performed with GraphPad Prism software (GPAD, version 5.0, San Diego, Calif.). The effects of LXR activation or human apoA-I expression on gross and plasma chemical parameters, kinetic studies, or levels of gene expression were determined either with a nonparametric Kruskal-Wallis test followed by a Dunn multiple comparison test or a parametric one-way ANOVA followed by a Newman-Keuls' multiple comparison test, as appropriate. The relationship between hepatic gene expression of abcg5/g8 and fecal excretion of [^{3}H]-cholesterol was tested with Spearman's correlation. Differences between groups were considered statistically significant when the P value was <0.05.

RESULTS

Gross and biochemical features of db/db mice. As expected, the body weights of db/db mice significantly increased with time and the obese phenotype was characterized by the accumulation of ectopic fat in several tissues, including the liver (Table I). A commensurate elevation in the gene expression of several targets of hepatic steatosis was also observed (Supplementary Table I). These mice displayed an insulin-resistant phenotype that consisted of hyperglycemia, hyperinsulinemia, and impaired glucose tolerance (Table I and Supplementary Table II).

The db/db mice had elevated plasma levels of total cholesterol, mostly attributed to increased plasma levels associated with the HDL fraction (Table I and Supplementary Fig 1, panel *A*). A detailed analysis of the HDL isolated by ultracentrifugation confirmed that the circulating amount of this group of lipoproteins was increased in db/db mice (Supplementary Table III). The electrophoretic analysis of plasma HDL further revealed that HDL particles were larger than those in Ctrl mice (Supplementary Fig 1, panels *B* and *C*), these particles were enriched in cholesteryl esters (Supplementary Table III). In this regard, a commensurate elevation (∼+1.5-fold; $P < 0.05$) in the plasma levels of LCAT was observed in db/db mice (236.5 ± 31.9 nmol mL^{-1} h^{-1}; n = 6) compared with Ctrl mice (162.0 ± 10.2 nmol mL^{-1} h^{-1}, n = 4). Although both the amount and size of HDL particles in db/db mice were elevated, plasma levels of mouse apoA-I did not differ between groups (Supplementary Fig 1, panel *D*), indicating an altered lipid/protein ratio in this class of lipoproteins. A significant increase in the plasma levels of phospholipid transfer protein activity (∼+1.8-fold; $P < 0.05$) was observed in db/db mice (33.3 ± 2.5 nmol mL^{-1} h^{-1}; n = 4) compared with that of Ctrl mice (18.2 ± 0.7 nmol mL^{-1} h^{-1}, n = 4). There was also an increased formation (∼+1.4-fold, $P < 0.05$) of preβ-HDL particles in the plasma of db/db compared with Ctrl mice (Supplementary Fig 1, panel *E*).

Impaired m-RCT in db/db mice. Abca1-independent cholesterol efflux to large HDL ex vivo was only moderately increased (∼+4%, $P < 0.05$) in db/db mice compared with nonobese mice (Supplementary Fig 1, panel *F*). Similarly, Abca1-dependent cholesterol efflux to smaller plasma acceptors (ie, preβ-HDL) from db/db was also moderately increased compared with those from nonobese mice. To ascertain the impact of the db/db phenotype on

Table I. General characterization of the db/db mice

Parameters	Ctrl	db/db	P
Mouse characteristics			
Initial weight [g]	26.4 ± 1.8	33.6 ± 6.4	<0.001
Final weight [g]	30.6 ± 0.9	50.7 ± 1.7	<0.001
Daily weight increase [g/d]	0.08 ± 0.03	0.37 ± 0.03	<0.001
Food intake [g/d]	3.5 ± 1.0	5.0 ± 0.4	<0.01
Water intake [mL/d]	8.4 ± 2.8	12.5 ± 2.6	<0.01
Total fat [g]	2.2 ± 0.2	13.5 ± 1.0	<0.001
Fat percentage vs body weight [%]	8.2 ± 0.4	27.6 ± 1.8	<0.001
Liver weight [g]	1.6 ± 0.1	4.6 ± 0.3	<0.001
Plasma biochemistry			
Glucose [mg/dL]	246.6 ± 5.5	540.2 ± 31.3	<0.001
Insulin [μg/L]	1.2 ± 0.2	55.9 ± 22.9	<0.001
ALT [U/L]	21.1 ± 1.7	119.1 ± 18.0	<0.001
AST [U/L]	68.7 ± 9.7	121.1 ± 34.0	<0.001
Cholesterol [mM]	2.2 ± 0.1	6.3 ± 0.1	<0.001
Free cholesterol [%]	30.8 ± 0.4	27.1 ± 0.3	ns
HDL-cholesterol [mM]	1.6 ± 0.0	5.1 ± 0.3	<0.001
Non-HDL cholesterol [mM]	0.6 ± 0.0	1.2 ± 0.1	<0.001
27-hydroxycholesterol [mg/dL]	0.010 ± 0.001	0.029 ± 0.006	<0.01
Liver biochemistry			
Cholesterol [μmol/liver]	5.3 ± 0.5	18.1 ± 4.4	<0.001
Triglycerides [μmol/liver]	5.1 ± 1.0	185.5 ± 24.1	<0.001
27-hydroxycholesterol [μg/g]	0.187 ± 0.047	0.627 ± 0.074	<0.01

Abbreviations: ALT, alanine transaminase; *AST*, aspartate transaminase; *Ctrl*, control mice; *db/db*, db/db mice; *HDL*, high-density lipoproteins; *non-HDL*, non-HDL fraction; *ns*, non significant.
Data are expressed as mean ± SE (n = 5 mice per group). Differences vs Ctrl were found significant at *P* values lower than 0.05, otherwise is indicated as ns. The plasma lipids associated to the HDL fraction were determined in the supernatants of plasma after precipitating the apoB-containing lipoproteins using phosphotungstic acid reagent (Roche). The non-HDL fraction (including apoB-containing lipoproteins) was obtained after subtracting the concentration of the lipid parameter calculated in the HDL fraction to that of total plasma.

m-RCT, radiolabeled cholesterol was loaded in macrophages and injected into mice. The db/db mice exhibited higher relative levels of plasma [^{3}H]-cholesterol compared with Ctrl mice (Fig 1, panel *A*), with counts primarily associated with the HDL fraction (Fig 1, panel *B*). The db/db mice also exhibited higher liver [^{3}H]-cholesterol counts 48 h after the injection of radiolabeled macrophages (Fig 1, panel *C*). However, [^{3}H]-tracer counts (both in the form of cholesterol and bile acids) in the feces of db/db mice were proportionally lower than those of Ctrl mice (Fig 1, panels *D–F*).

Defective HDL turnover in db/db mice. Mice from each group were injected intravenously with HDL-containing [^{3}H]-cholesteryl oleate. Radiolabeled HDL from db/db mice showed a delayed turnover compared with nonobese mice (Fig 2); the fractional catabolic rate was approximately half that of Ctrl mice. When injected into Ctrl mice, the [^{3}H]-HDL from db/db ($HDL_{db/db}$) was cleared as fast as those from nonobese mice (Supplementary Table IV). Consistently, gene expression of *Scarb1*, which encodes SR-BI, the main receptor involved in the cholesteryl ester uptake, was repressed in the liver in db/db mice (Supplementary Table I). As in the case of m-RCT analysis, db/db mice displayed higher liver [^{3}H]-cholesterol ester counts 48 hours after [^{3}H]-HDL injection but lower [^{3}H]-tracer counts (both in the form of cholesterol and bile acids) in feces compared with Ctrl mice (Fig 2). Similar results were observed in independent experiments that evaluated the fate of oral gavaged [^{3}H]-cholesterol over a period of 48 hours (Supplementary Fig 2).

LXR signaling is impaired in the liver of db/db mice. The gene expression of several LXR targets was downregulated in the liver in db/db mice (Table II), including several members of the ABC transporters family (ie, *Abcga1*, *Abcg1*, *Abcg5*, and *Abcg8*), as well as other targets involved in the classical (ie, *Cyp7a1*) or alternate pathway (ie, *Cyp27a1*) of bile acid synthesis (Supplementary Table I). Importantly, the expression of hepatic *Nr1h3* mRNA, which encodes LXRα itself, was also found to be significantly reduced in db/db mice (Table II). In particular, the reduced hepatic levels of *Abcg5/g8* mRNA might explain the retention of cholesterol in this organ. Interestingly, the hepatic levels of 27-hydroxycholesterol, a known representative of endogenous LXR agonists, were

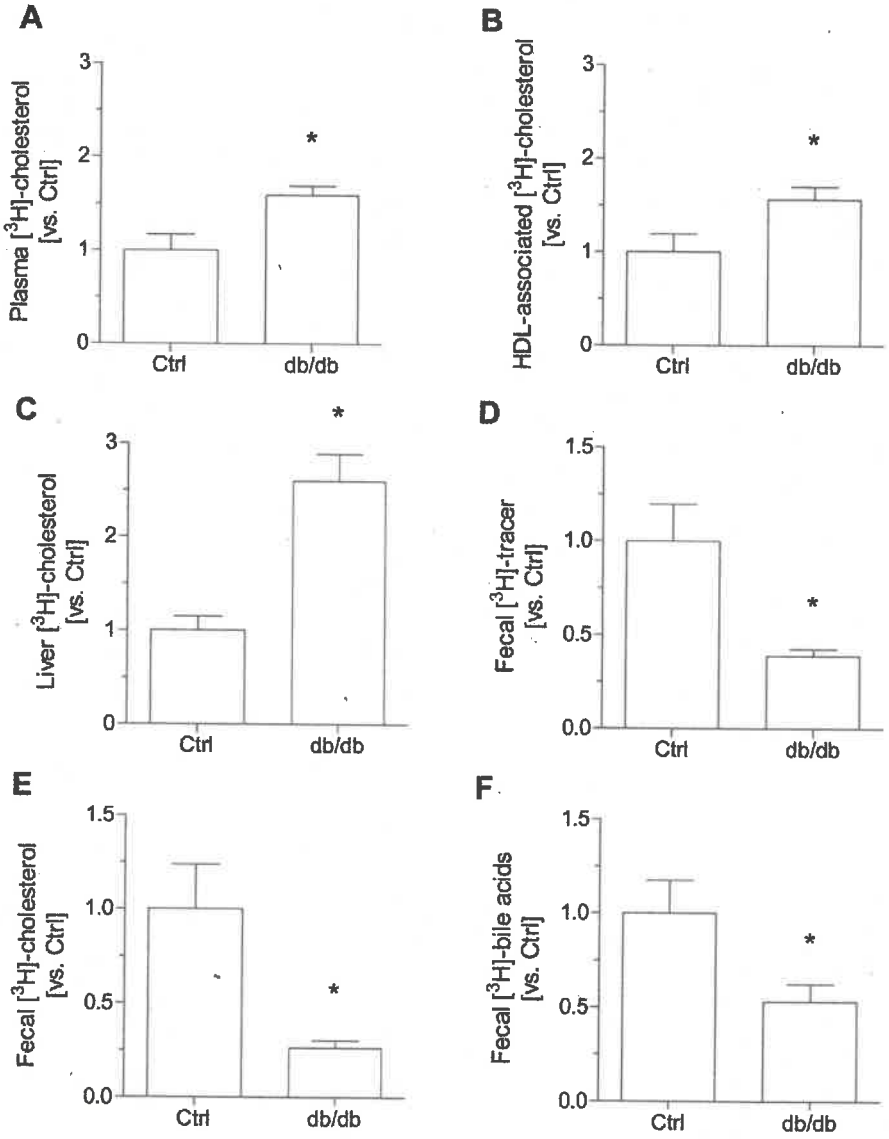

Fig 1. m-RCT in vivo. Macrophage-to-plasma m-RCT was increased in db/db mice, but liver-to-feces m-RCT was differentially modulated and dependent on the mice. Individually housed mice were injected i.p. with [^{3}H]-cholesterol-labeled J774 mouse macrophages, and the distribution of counts into different compartments was determined 48 h after injection. In all panels, results are the mean ± SE of 5 mice and are expressed as fold increase, taking as the reference the % vs injected dose determined in Ctrl mice (vs Ctrl). **A,** Total plasma levels of [^{3}H]-cholesterol (Ctrl: 0.91% ± 0.11% vs injected dose). **B,** plasma levels of [^{3}H]-cholesterol in the HDL fraction (Ctrl: 0.61% ± 0.07% vs injected dose). **C,** hepatic levels of [^{3}H]-cholesterol (Ctrl: 1.90% ± 0.27% vs injected dose). **D,** fecal [^{3}H]-tracer (Ctrl: 0.17% ± 0.03% vs injected dose). **E,** fecal [^{3}H]-cholesterol (Ctrl: 0.10% ± 0.02% vs injected dose). **F,** fecal [^{3}H]-biliary acids (Ctrl: 0.08% ± 0.01% vs injected dose). Differences vs Ctrl were found to be significant at P values lower than 0.05. Ctrl, control mice; db/db, db/db mice. *$P < 0.05$ vs control (Ctrl) mice.

significantly increased in both liver (>+3-fold, $P < 0.05$) and plasma (~+3-fold, $P < 0.05$) samples from db/db mice (Table I).

Pharmacologic induction of LXR partly restores m-RCT in db/db mice. The reduced levels of several hepatic LXR targets, particularly those controlling hepatobiliary cholesterol trafficking, that is, Abcg5/g8, might be attributed to impaired LXR function, which in turn would partly explain the impaired m-RCT found in db/db mice. Therefore, we used a specific LXR agonist (ie, T0901317) and analyzed its impact on the m-RCT of db/db mice.

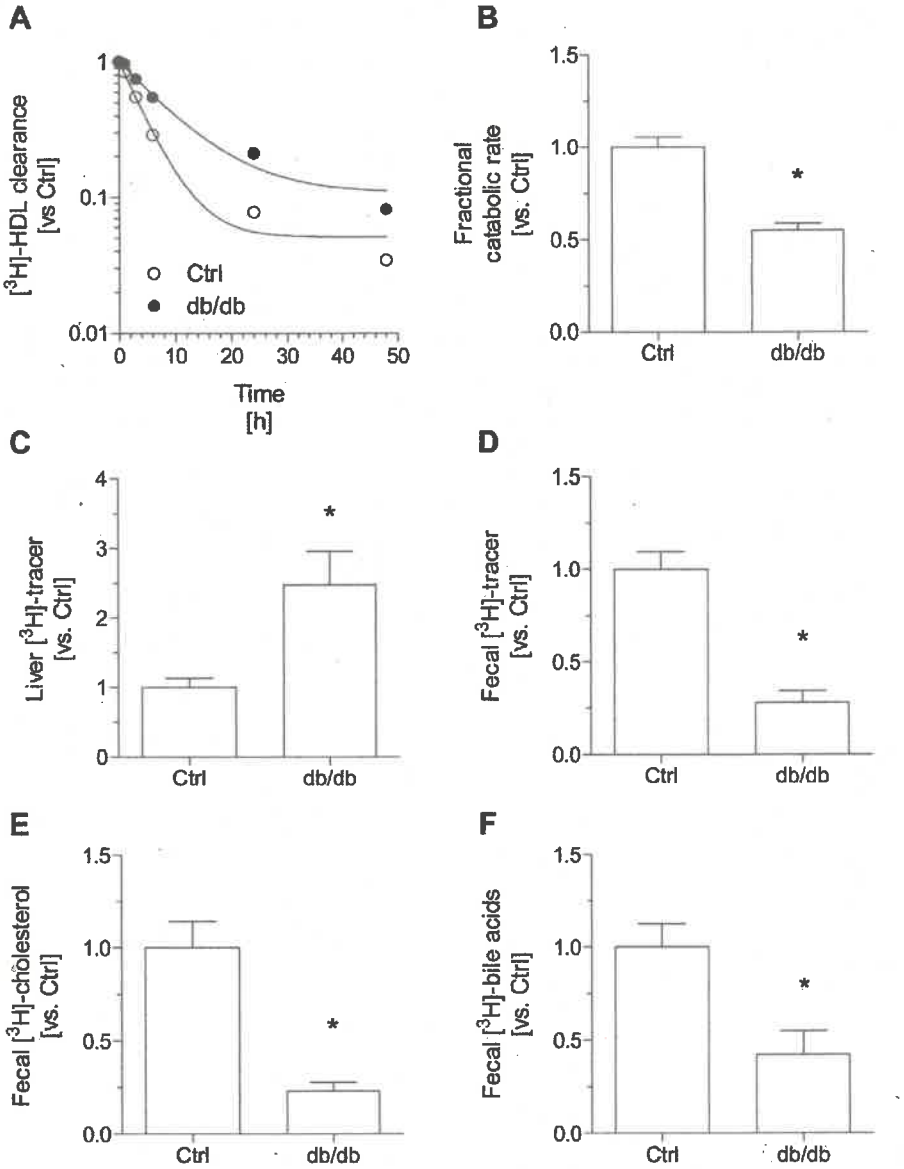

Fig 2. HDL kinetics. Autologous HDL was isolated from pooled mouse plasma, labeled with [^{3}H]-cholesteryl oleate, and injected intravenously into mice. The radioactivity of HDL in blood 2 min postinjection was defined as 1, its decay was monitored in plasma at the times indicated, and its distribution in liver and feces was measured 48 h after injection. The fractional catabolic rate was calculated with data points for 48 h. **A,** turnover data in plasma are expressed as a fraction of the injected dose. **B,** fractional catabolic rate of HDL cholesterol (pools/h) of each genotype. **C,** HDL-derived [^{3}H]-cholesteryl oleate in the liver. **D,** in vivo excretion of HDL-derived [^{3}H]-cholesteryl oleate in feces. **E,** HDL-derived [^{3}H]-cholesteryl oleate in fecal cholesterol. **F,** HDL-derived [^{3}H]-cholesteryl oleate in fecal bile acids. In **B–F,** results are the mean ± SE of 5 mice. Differences vs Ctrl were found to be significant at P values lower than 0.05. Ctrl, control mice; db/db, db/db mice. *$P < 0.05$ vs control (Ctrl) mice.

LXR agonist administration to mice did not affect body or liver weight of either db/db or Ctrl mice (Table III). LXR induction produced an elevation in HDL-C plasma levels in both db/db mice (db/db-LXR) and their nonobese littermates (Ctrl-LXR) compared with their untreated counterparts (Table III). Hepatic levels of cholesterol and triglycerides were also elevated in response to LXR agonist treatment (Table III). This was also the case regarding the gene expression of known LXR targets, particularly those relevant to the hepatobiliary transport of cholesterol, that is, Abcg5/g8 (Table IV).

Table II. Liver-related expression profile of genes involved in HDL metabolism and m-RCT

Genes	Ctrl	db/db	P
Abca1 [vs Ctrl]	1.0 ± 0.1	0.3 ± 0.1	<0.01
Abcg1 [vs Ctrl]	1.0 ± 0.2	0.4 ± 0.1	<0.05
Abcg5 [vs Ctrl]	1.0 ± 0.1	0.5 ± 0,1	<0.01
Abcg8 [vs Ctrl]	1.0 ± 0.1	0.4 ± 0.1	<0.001
Cyp7a1 [vs Ctrl]	1.0 ± 0.4	0.4 ± 0.1	<0.01
Nr1h3 [vs Ctrl]	1.0 ± 0.1	0.4 ± 0.1	<0.001

Abbreviations: Ctrl, control mice; *db/db*, db/db mice.
Data are expressed as mean ± SE (n = 5). Differences vs Ctrl were found significant at *P* values lower than 0.05.

The db/db-LXR mice exhibited higher plasma levels of [^{3}H]-cholesterol after the injection of radiolabeled macrophages compared with the untreated, db/db mice, which was mainly associated with HDL (Fig 3). As in the case of untreated, db/db mice, db/db-LXR mice also showed elevated hepatic levels of [^{3}H]-cholesterol, which was mostly attributed to free cholesterol (Supplementary Table V). In contrast, [^{3}H]-tracer levels (in the form of cholesterol) were significantly higher in feces of db/db-LXR mice compared with untreated, db/db mice, with values close to those observed in untreated, Ctrl mice (Fig 3). Consistently, both mRNA and protein levels of Abcg5 and Abcg8 in the liver in db/db-LXR mice reached levels similar to those observed in untreated, Ctrl mice (Fig 4, panels *A–D*; Supplementary Fig 3). It is noteworthy that the relative hepatic levels of *Abcg5* and *Abcg8* were directly related to fecal [^{3}H]-cholesterol excretion (*Abcg5*: Spearman's r = +0.63; $P < 0.01$; *Abcg8*: Spearman's r = +0.59; $P < 0.01$) (Fig 4, panels *E* and *F*).

The induction of the LXR signaling on the expression of different cholesterol transporters was also evident in the small intestine (Fig 5). For instance, the gene expression of *Abca1* and *Abcg1* in this tissue was induced by the LXR agonist either in both Ctrl (*Abca1*: ∼+2.6-fold vs untreated, Ctrl mice, $P < 0.05$; *Abcg1*: ∼+2.2-fold vs untreated, Ctrl mice, $P < 0.05$, respectively) and db/db mice (*Abca1*: ∼+3.9-fold vs untreated, db/db mice, $P < 0.05$; *Abcg1*: ∼+2.9-fold vs untreated, db/db mice, $P < 0.05$, respectively) (Fig 5, panels *A* and *B*). Consistently, the gene expression of *Abcg5* and *Abcg8* in the small intestine was also upregulated by the LXR agonist either in both Ctrl (*Abcg5*: ∼+1.7-fold vs untreated, Ctrl mice, $P < 0.05$; *Abcg8*: ∼+2.1-fold vs untreated, Ctrl mice, $P < 0.05$, respectively) and db/db mice (*Abcg5*: ∼+1.4-fold vs untreated, db/db mice, $P < 0.05$; *Abcg8*: ∼+1.9-fold vs untreated, db/db mice, $P < 0.05$, respectively) (Fig 5, panels *C* and *D*). Similarly to the liver, the relative intestinal levels of *Abcg5* and *Abcg8* were also directly related to fecal [^{3}H]-cholesterol excretion (*Abcg5*: Spearman's r = +0.67; $P < 0.01$; *Abcg8*: Spearman's r = +0.53; $P < 0.05$) (Fig 5, panels *E* and *F*). No changes were observed in the gene expression of *Npc1l1* (data not shown).

Upregulation of ABCG5 and ABCG8 in liver from morbidly obese patients after bariatric surgery. We evaluated the impact of surgery on the relative abundance of hepatic *ABCG5* and *ABCG8* mRNA in a small cohort of morbidly obese patients. Compared with baseline, hepatic levels of *ABCG5* and *ABCG8* mRNA were

Table III. Impact of LXR agonist administration on mouse parameters

Parameters	Ctrl	db/db	Ctrl-LXR	db/db-LXR	P
Mouse characteristics					
Body weight [g]	29.4 ± 0.8	48.1 ± 1.2*	28.8 ± 0.8	46.2 ± 0.9*‡	<0.001
Liver weight [g]	1.5 ± 0.1	4.5 ± 0.4*	1.3 ± 0.1	4.4 ± 0.3*‡	<0.01
Food intake [g/d]	2.4 ± 0.1	9.5 ± 0.5*	4.7 ± 0.1*	9.2 ± 1.0*‡	<0.01
Water intake [mL/d]	13.3 ± 0.9	26.8 ± 1.3*	22.1 ± 1.8*	36.4 ± 2.1*†‡	<0.01
Plasma biochemistry					
Cholesterol [mM]	2.6 ± 0.1	5.6 ± 0.3*	3.8 ± 0.2*	7.3 ± 0.9*‡	<0.001
HDL-cholesterol [mM]	2.0 ± 0.2	4.3 ± 0.4*	3.0 ± 0.2*	6.0 ± 0.7*‡	<0.001
Non-HDL cholesterol [mM]	0.7 ± 0.1	1.5 ± 0.4*	0.8 ± 0.1	1.1 ± 0.4	<0.05
Liver biochemistry					
Total cholesterol [μmol/liver]	6.0 ± 1.0	33.3 ± 4.4*	9.1 ± 0.3*	24.0 ± 4.5*‡	<0.01
Total triglyceride [μmol/liver]	9.2 ± 2.6	197.6 ± 54.9*	94.0 ± 20.7*	320.7 ± 29.8*†‡	<0.01

Abbreviations: Ctrl, control mice; *db/db*, db/db mice; *Ctrl-LXR*, LXR agonist-treated Ctrl mice; *db/db-LXR*, LXR agonist-treated db/db mice.
Results are expressed as the means ± SE (n = 4–7 mice per group). Plasma levels of the HDL fractions were determined in the plasma supernatants after precipitating with phosphotungstic acid; the non-HDL fraction was calculated by subtracting the HDL moiety to the total plasma. When indicated, mice were treated with the LXR agonist (T0901317) at a dose of 20 mg per kg of body weight during 10 consecutive days. Differences between the mean values were assessed by the nonparametric Kruskal-Wallis test followed by Dunn's post-test or ANOVA followed a Newman-Keuls post-test, as appropriate; differences were considered significant when $P < 0.05$. Specifically, *$P < 0.05$ vs untreated Ctrl group; †$P < 0.05$ vs untreated db/db group; or ‡$P < 0.05$ vs LXR agonist-treated Ctrl mice.

Table IV. Liver-related expression profile of gene targets of LXR

Genes	Ctrl	db/db	Ctrl-LXR	db/db-LXR	*P*
Abca1 [vs Ctrl]	1.0 ± 0.1	0.6 ± 0.0*	1.4 ± 0.3	1.1 ± 0.1†	<0.001
Abcg5 [vs Ctrl]	1.0 ± 0.1	0.5 ± 0.1*	2.3 ± 0.5*	0.7 ± 0.1‡	<0.001
Abcg8 [vs Ctrl]	1.0 ± 0.1	0.4 ± 0.1*	1.3 ± 0.2*	0.7 ± 0.1†‡	<0.001

Abbreviations: Ctrl, untreated control mice; *db/db*, untreated db/db mice; *Ctrl-LXR*, LXR agonist-treated Ctrl mice; *db/db-LXR*, LXR agonist-treated db/db mice.
Results are expressed as the means ± SE (n = 4–7 mice per group). When indicated, mice were treated with the LXR agonist (ie, T0901317) at a dose of 20 mg per kg of body weight during 10 consecutive days. Differences between mean values were assessed by the nonparametric Kruskal-Wallis test followed by Dunn's post-test or ANOVA followed by a Newman-Keuls post-test, as appropriate; differences were considered significant when $P < 0.05$. Specifically, *$P < 0.05$ vs untreated Ctrl group; †$P < 0.05$ vs untreated db/db group; or ‡$P < 0.05$ vs LXR agonist-treated Ctrl mice.

upregulated (*ABCG5*: ~+1.9-fold, $P < 0.05$; *ABCG8*: ~+1.5-fold, $P < 0.05$, respectively) 12 mo. after surgery (Fig 6, panels *A* and *B*). Similarly, the gene expression of other known targets of LXRα (ie, *ABCA1* and *ABCG1*) and *NR1H3*, which codifies LXRα itself, was also upregulated (*NR1H3*: ~+1.9-fold, $P < 0.01$; *ABCA1*: ~+1.3-fold, $P < 0.01$; *ABCG1*: ~+1.4-fold, $P < 0.01$) following this intervention (Fig 6, panels *C–E*). The hepatic gene expression of *NR1H2*, which codifies LXRβ, was also induced (*NR1H2*: ~+1.4-fold, $P < 0.01$) after bariatric surgery (Fig 6, panel *F*). This gene expression profile was concomitant with an improvement in hepatic lipid levels (Supplementary Table VI).

DISCUSSION

The leptin receptor–deficient mouse (db/db) has been a suitable model with which to study the influence of leptin in regulating the abundance of Abcg5/g8 protein.[9] However, the molecular mechanisms by which leptin controls hepatic Abcg5/g8 protein levels remain poorly understood. Moreover, the contribution of metabolic abnormalities occurring in response to insulin resistance and fat accumulation in the liver in different models of obesity often complicates the interpretation of studies.

Our data reveal that m-RCT into feces was significantly reduced in db/db mice compared with nonobese mice; the latter finding was consistent with a previous study that used the same mice.[8] However, the pattern of radiolabel compartment distribution significantly differed from that observed in the present work. For instance, our data show that the [^{3}H]-tracer accumulates in HDL and in the livers of db/db mice, whereas in the former study,[8] impaired m-RCT was mainly attributed to a decreased uptake of [^{3}H]-cholesterol by plasma acceptors and lower levels of [^{3}H]-tracer in the liver. However, Low et al. (2012) did not analyze the gene expression of targets involved in liver cholesterol trafficking. They suggested that undetermined tissue-specific factors contributed to the observed phenotype. We speculate that the differences between our studies might be explained, at least in part, by genetic background–specific variability between the db/db mouse models used (ie, C57BKS/J vs C57BL/6J).

Our db/db mice had more cholesterol on larger HDL lipoproteins and had a higher potential to generate preβ-HDL particles. However, this change was not associated with a higher Abca1-dependent cholesterol efflux to apoB-depleted plasma, thereby suggesting that the relatively higher proportion of [^{3}H]-cholesterol in plasma during m-RCT might be rather attributable to increased plasma levels of HDL-C. Likewise, such elevated levels of plasma HDL-C would also account for the increase in cholesterol efflux to large HDL observed ex vivo, indicating that the macrophage-to-plasma component is not a major rate-limiting determinant of in vivo m-RCT in db/db mice. In contrast, our data revealed the hepatic retention of [^{3}H]-cholesterol concomitant with a reduced output of the tracer into feces, thus indicating that the liver-to-gut component of m-RCT is impaired in db/db mice. Other mice with defects in the leptin axis (ie, either db/db or ob/ob mice) have also shown lower levels of biliary cholesterol compared with their nonobese littermates.[9,30,31] In our study, the obese phenotype of db/db mice was accompanied by a significant reduction in the hepatic levels of both Abcg5/g8 mRNA and protein. The regulation of the hepatic expression of Abcg5/g8 is complex. Although reductions in hepatic levels are generally present in mice that lack a functional leptin axis, the mechanism by which leptin controls Abcg5/g8 levels is still not completely known. Recent evidence supports the notion that leptin signaling might not directly regulate hepatic expression.[32] In this regard, decreased hepatic expression of Abcg5/g8 in leptin-deficient (ob/ob) mice has been associated with altered endoplasmic reticulum function, which is the site of Abcg5/g8 complex assembly.[33,34] Our data revealed that, in addition to

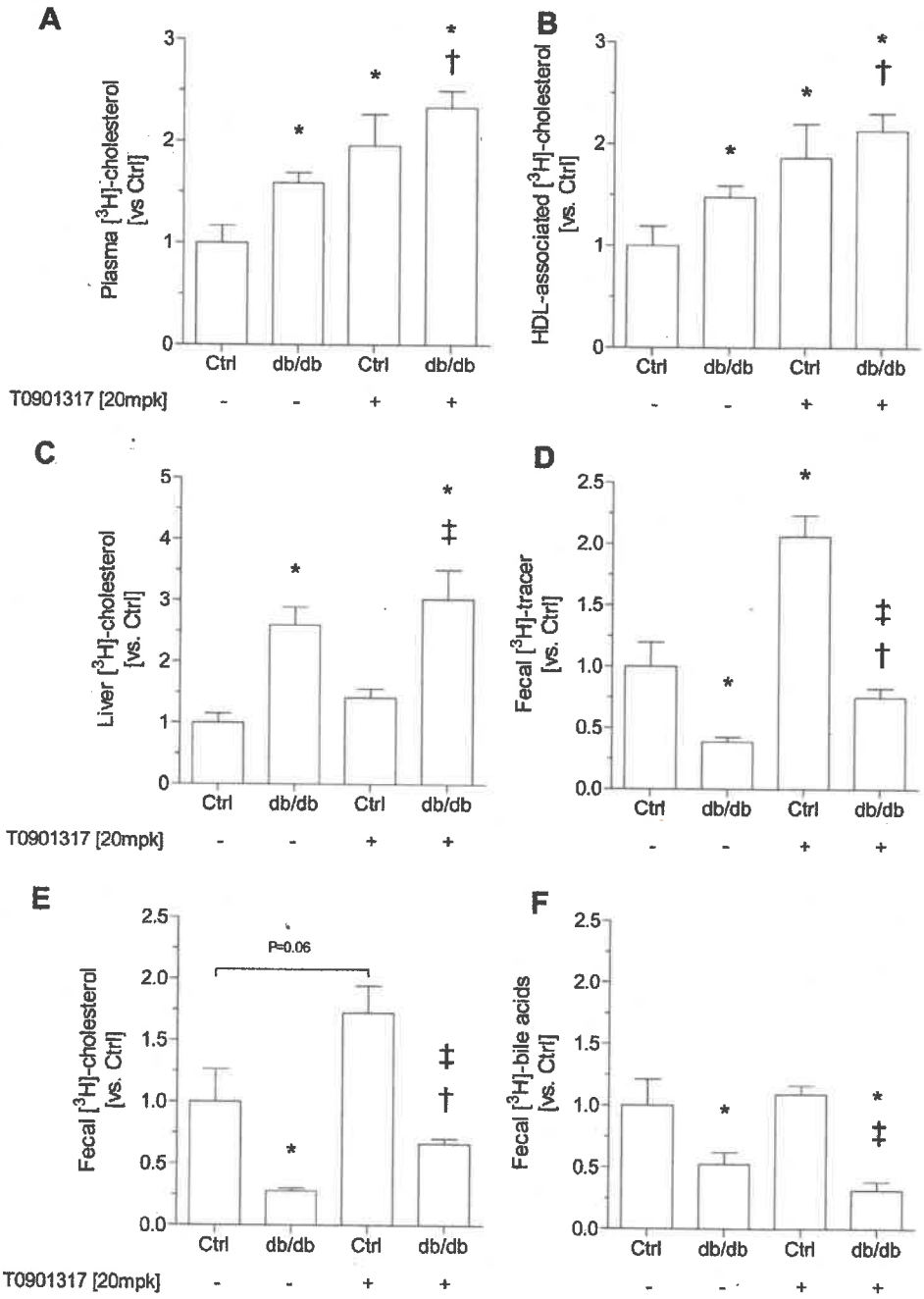

Fig 3. LXR promotes m-RCT in vivo. Macrophage-to-plasma m-RCT was increased in db/db mice, but liver-to-feces m-RCT was partly rescued via treatment with an LXR agonist. Individually housed mice were injected i.p. with [^{3}H]-cholesterol-labeled J774 mouse macrophages, and the distribution of counts into different compartments was determined 48 h after the injection. Mice (either db/db or their littermates) were matched for body weight and randomized into 2 groups and were treated with daily intragastric doses of either T0901317 (20 mg/kg; ie, Ctrl-LXR and db/db-LXR) or a vehicle solution for 10 days. In all panels, results are the mean ± SE of 4–7 mice and are expressed in fold increase, taking as a reference the % vs injected dose determined in Ctrl mice (vs Ctrl). **A,** total plasma levels of [^{3}H]-cholesterol (Ctrl: 1.3% ± 0.2% vs injected dose). **B,** plasma levels of [^{3}H]-cholesterol in the HDL fraction (Ctrl: 0.7% ± 0.1% vs injected dose). **C,** hepatic levels of [^{3}H]-cholesterol (Ctrl: 2.5% ± 0.4% vs injected dose). **D,** fecal [^{3}H]-tracer (Ctrl: 0.18% ± 0.04% vs injected dose). **E,** fecal [^{3}H]-cholesterol (Ctrl: 0.11% ± 0.03% vs injected dose). **F,** fecal [^{3}H]-bile acids (Ctrl: 0.07% ± 0.02% vs injected dose). Differences between mean values were assessed by the nonparametric Kruskal-Wallis test followed by Dunn's post-test or ANOVA followed by a Newman-Keuls post-test, as appropriate; differences were considered significant when P was <0.05. Specifically, *$P < 0.05$ vs untreated control (Ctrl) mice; †$P < 0.05$ vs untreated db/db mice; or ‡$P < 0.05$ vs LXR agonist-treated Ctrl mice. Ctrl, untreated control mice; db/db, untreated db/db mice; Ctrl-LXR, LXR agonist-treated Ctrl mice; db/db-LXR, LXR agonist-treated db/db mice.

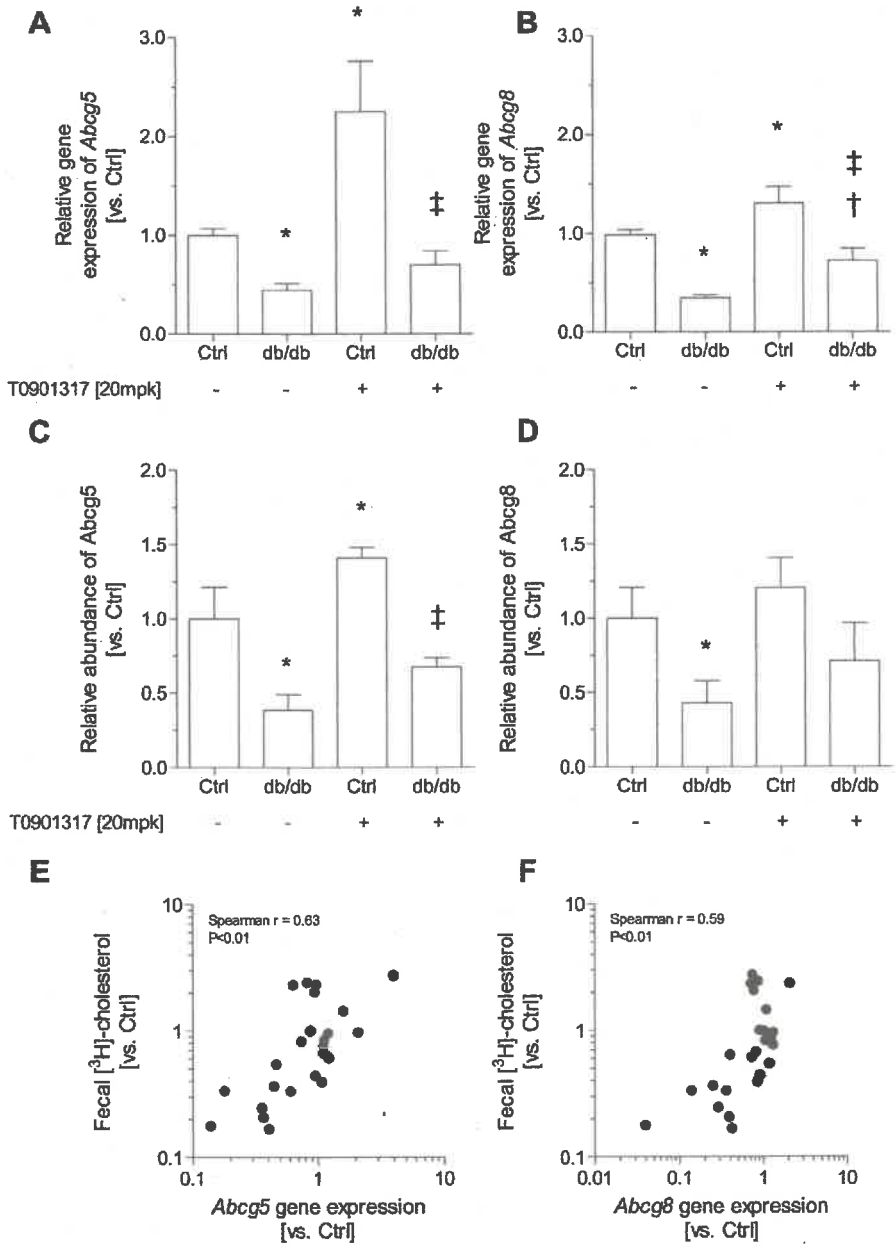

Fig 4. Effects of LXR agonists on relevant hepatic cholesterol transporters. Mice (either db/db or their littermates) were matched for body weight and randomized into 2 groups and were treated with daily intragastric doses of either T0901317 (20 mg/kg; ie, Ctrl-LXR and db/db-LXR) or a vehicle solution for 10 days. **A,** relative gene expression of *Abcg5*. **B,** relative gene expression of *Abcg8*. **C,** relative protein abundance of Abcg5. **D,** relative gene expression of Abcg8. **E,** Spearman correlation between the relative gene expression of *Abcg5* and the fecal excretion of [^{3}H]-cholesterol. **F,** Spearman correlation between the relative gene expression of Abcg8 and the fecal excretion of [^{3}H]-cholesterol. In all panels, results are the mean ± SE of 4–7 mice and are expressed as fold increase, taking as a reference the % vs injected dose determined in Ctrl mice (vs Ctrl). In **C** and **D,** data from the densitometric analysis of 4 animals are shown. Differences between mean values were assessed by the nonparametric Kruskal-Wallis test followed by Dunn's post-test or ANOVA followed by Newman-Keuls post-test, as appropriate; differences were considered significant when P was <0.05. Specifically, *$P < 0.05$ vs untreated control (Ctrl) mice; †$P < 0.05$ vs untreated db/db mice; or ‡$P < 0.05$ vs LXR agonist-treated Ctrl mice. Ctrl, untreated control mice; db/db, untreated db/db mice; Ctrl-LXR, LXR agonist-treated Ctrl mice; db/db-LXR, LXR agonist-treated db/db mice.

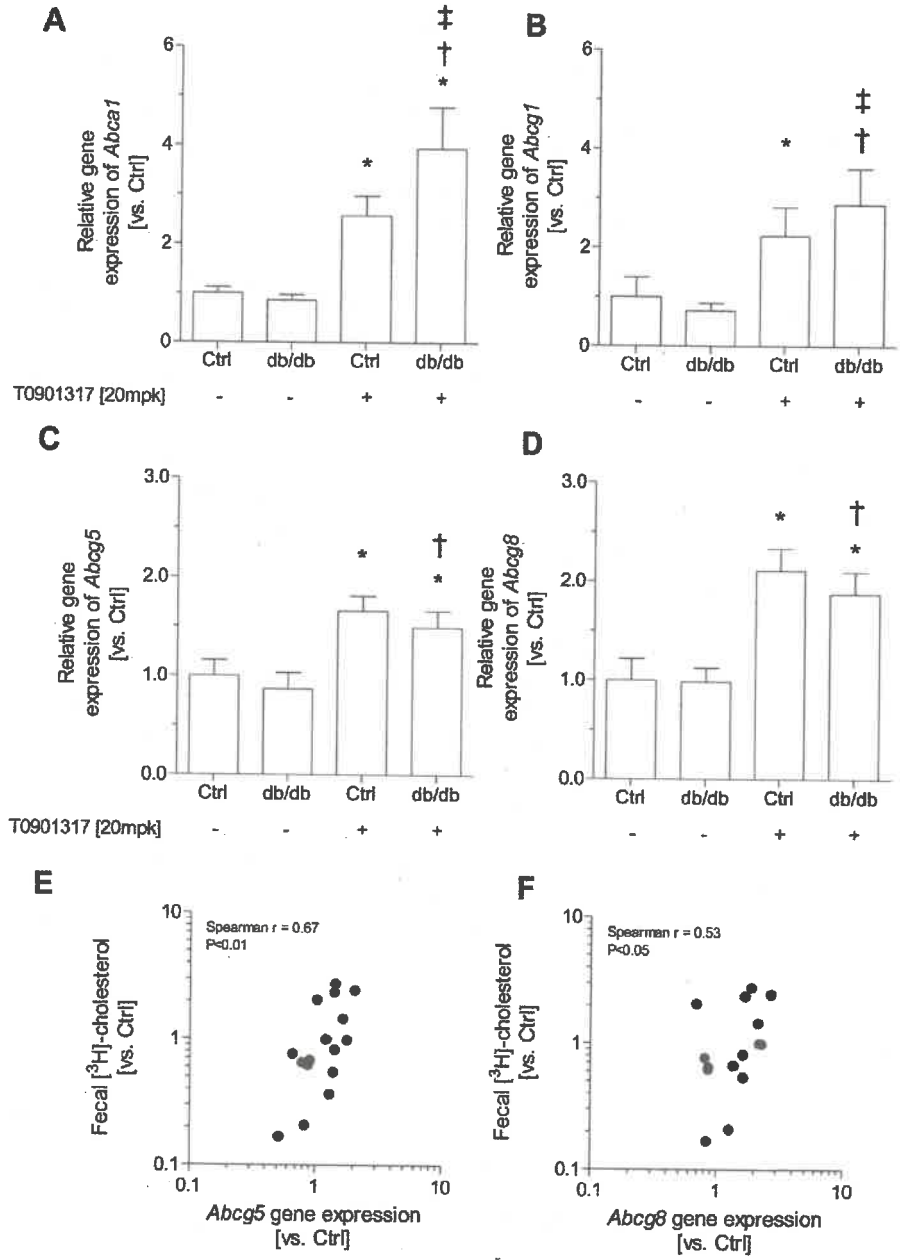

Fig 5. Effects of LXR agonists on relevant small intestine cholesterol transporters. Mice (either db/db or their littermates) were matched for body weight and randomized into 2 groups and were treated with daily intragastric doses of either T0901317 (20 mg/kg; ie, Ctrl-LXR and db/db-LXR) or a vehicle solution for 10 days. **A,** relative gene expression of *Abca1*. **B,** relative gene expression of *Abcg1*. **C,** relative gene expression of *Abcg5*. **D,** relative gene expression of *Abcg8*. **E,** Spearman correlation between the relative gene expression of *Abcg5* and the fecal excretion of [^{3}H]-cholesterol. **F,** Spearman correlation between the relative gene expression of *Abcg8* the fecal excretion of [^{3}H]-cholesterol. In all panels, results are the mean ± SE of 4 mice and are expressed as fold increase, taking as a reference the % vs injected dose determined in Ctrl mice (vs Ctrl). Differences between mean values were assessed by the nonparametric Kruskal-Wallis test followed by Dunn's post-test or ANOVA followed by Newman-Keuls post-test, as appropriate. Differences were considered significant when P was <0.05. Specifically, *$P < 0.05$ vs untreated control (Ctrl) mice; †$P < 0.05$ vs untreated db/db mice; or ‡$P < 0.05$ vs LXR agonist-treated Ctrl mice. Ctrl, untreated control mice; db/db, untreated db/db mice; Ctrl-LXR, LXR agonist-treated Ctrl mice; db/db-LXR, LXR agonist-treated db/db mice.

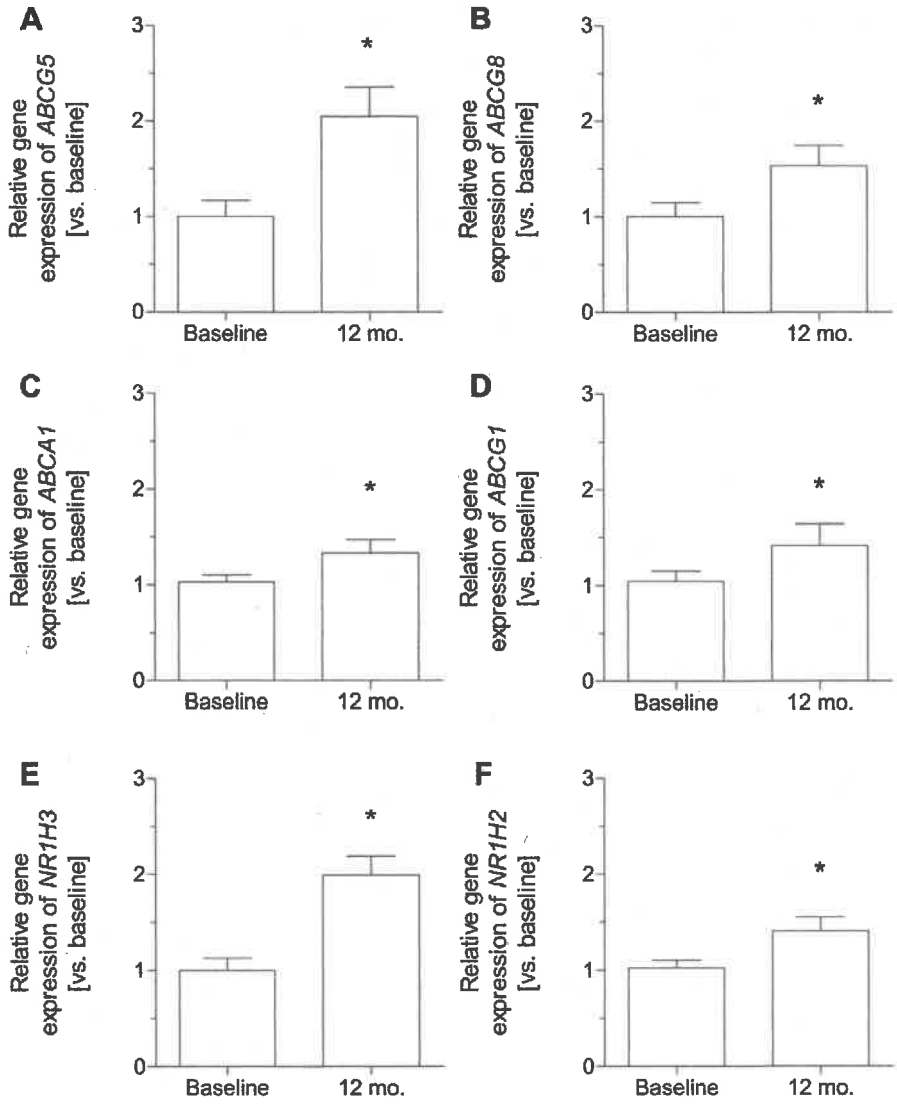

Fig 6. Effect of bariatric surgery on hepatic gene expression of cholesterol transporters and LXR in morbidly obese patients. Results are expressed as the mean ± SE (n = 10). Values are represented as fold change vs baseline. **A,** *ABCG5*. **B,** *ABCG8*. **C,** *ABCA1*. **D,** *ABCG1*. **E,** *NR1H3* and **F,** *NR1H2*. A nonparametric Wilcoxon's test was used for paired values. Differences vs baseline were found to be significant at *P* values lower than 0.05. $*P < 0.05$ vs baseline.

Abcg5/g8, the hepatic expression of other known gene targets of LXR was also significantly downregulated in db/db mice. Consistent with previous reports,[35] hepatic LXR signaling was found to be impaired in db/db mice despite the elevated hepatic levels of 27-hydroxycholesterol, a representative of the natural LXR ligands. It should be noted that in certain pathologic conditions that lead to an increased concentration of oxysterols, their sulfation could be considered a counter-regulatory mechanism. Therefore, taking into account that sulfated oxysterols might inhibit nuclear receptor signaling[36] and compete with endogenous LXR ligands, potentially its accumulation in the liver could explain, at least in part, the attenuated LXR signaling in the livers of db/db mice. However, m-RCT was stimulated by a synthetic high-affinity LXR agonist that is known to induce liver steatosis. This effect was mainly associated with a higher fecal [^{3}H]-cholesterol excretion, but not in bile acid excretion since the latter is controlled by different transporters and has an enhanced turnover in mice.[37] This finding is directly related to the hepatic gene expression of *Abcg5/g8* in

mice and indicates that a potent LXR activator that circumvents the undesired effects on hepatic triglyceride accumulation could constitute a potential therapeutic approach for correcting the m-RCT pathway in obesity. Taken together, our data strongly indicate that altered leptin signaling could affect the LXR-dependent regulation of Abcg5/g8 and consequently contribute to m-RCT impairment.

Of note, the induction of fatty liver in diet-induced obesity mice (without a leptin signaling deficiency) was concomitant with elevated levels of *Abcg5/g8* expression in the liver and enhanced fecal [^{3}H]-cholesterol excretion,[38] possibly due to the induction of LXR by the high cholesterol content of the diet. These changes were also found when mice were fed a high-cholesterol and cholate-containing diet, which induced severe fatty liver accumulation (Escolà-Gil, unpublished data), thus indicating that liver damage and defective LXR signaling are not always associated. Further supporting these observations, hepatic insulin resistance, a metabolic dysfunction frequently associated with fatty liver,[39] as induced by the tissue-specific deletion of the insulin receptor, has also been reported to promote biliary cholesterol excretion and upregulation of *Abcg5/g8*.[40]

Importantly, the expression of the Abcg5/g8 gene in the liver of a cohort of morbidly obese patients was upregulated postoperatively. This change was concomitant with the well-known significant amelioration of both obesity and hepatic steatosis after bariatric surgery. Plasma levels of leptin are elevated in obese individuals and are frequently associated with hepatic steatosis both in humans[41] and mice.[42] In this setting, leptin signaling might be impaired as a result of leptin resistance.[43] Therefore, the gene expression of *Abcg5/g8* in the liver could reflect an improved leptin response. In this context, plasma levels of leptin in morbidly obese patients were elevated (~+7-fold; $P < 0.001$) at baseline (35 ± 4 ng/mL) compared with levels 12 months after surgery (5 ± 1 ng/mL). Interestingly, the gene expression of *NR1H3* in the liver was also significantly enhanced in obese patients postoperatively, further revealing alterations in the LXR signaling in morbidly obese patients and supporting the concept of a cross-talk with leptin signaling in humans. These data also suggest that changes in gene expression shown in response to surgery would exert a favorable effect on the amelioration of m-RCT in obese patients.

Overall, our data are consistent with previous reports[37,44-48] in that hepatic Abcg5/g8 is required for biliary cholesterol secretion and fecal excretion of [^{3}H]-cholesterol. In support of this view, Abcg5/g8 upregulation has also been associated with increased biliary cholesterol excretion,[40,48] whereas Abcg5/g8 deficiency blocks hepatobiliary cholesterol excretion.[10,34,47,48] A genetic deficiency in Abcg5/g8 has also been reported to promote diet-induced obesity and hepatic steatosis in mice,[34] thus suggesting that impairment of this pathway strengthens disease development.

Related to m-RCT and as expected,[20] upregulation of LXR-responsive genes was also apparent in small intestine from mice treated with the LXR agonist T0901317. Abcg5 and Abcg8 are also expressed at significant levels in the enterocytes[49] and mediate the efflux of cholesterol from them into gut lumen.[20] The gene expression of these 2 cholesterol transporters in the small intestine was unchanged in db/db mice, but was significantly upregulated on treatment with the LXR agonist,[50] suggesting that their upregulation contributes to the enhanced [^{3}H]-cholesterol excretion into feces of db/db mice treated with LXR agonist.

In conclusion, our findings demonstrate that hepatic downregulation of Abcg5/g8 expression was closely associated with impaired macrophage-to-feces m-RCT in leptin receptor–deficient mice. m-RCT was partly restored by a potent LXR agonist partly by inducing the expression of Abcg5/g8 in both the liver and small intestine of these mice. Of note, these alterations in hepatic *ABCG5/G8* were also found in morbidly obese patients and were favorably regulated after Roux-en-Y gastric bypass surgery.

ACKNOWLEDGMENTS

Conflict of Interest: All authors have read the journal's policy on disclosure of potential conflicts of interest and have none to declare.

This work was partly funded by the Ministerio de Sanidad y Consumo, Instituto de Salud Carlos III (ISCIII) FIS grants CP13/00070 (to JJ), PI16/00139 (to JCE-G), PI11/01159 (to JP-O), PI11/01076 and PI12/0226 (to FB-V), PI15/01983 (to AC), PI13/02507 (to LB-R), and FEDER "Una manera de hacer Europa"; and by LaMarató 2016 (303/C/2016) (201602-31) (to JJ). JJ is a recipient of a Miguel Servet Type 1 contract (CP13/00070; ISCIII). TLE is a recipient of an FIS grant contract PI12-0226 (ISCIII). KAM-L is a recipient of an AGAUR grant FI-DGR2014 (Generalitat de Catalunya). CIBER de Diabetes y Enfermedades Metabólicas Asociadas (CIBERDEM) and CIBER de Enfermedades Cardiovasculares (CIBERCV) are projects of the Instituto de Salud Carlos III. The English grammar and language was corrected by American Journal Experts (www.aje.com). Institut de Recerca de l'Hospital de la Santa Creu i Sant Pau is accredited by the Generalitat de Catalunya as Centre de Recerca de Catalunya

(CERCA). The authors are very grateful to Annabel García León, Esther Cubero, Júlia Freixa, and Sari Nuutinen for technical assistance.

REFERENCES

1. Bays HE, Toth PP, Kris-Etherton PM, et al. Obesity, adiposity, and dyslipidemia: a consensus statement from the National Lipid Association. J Clin Lipidol 2013;7:304–83.
2. Tchernof A, Despres JP. Pathophysiology of human visceral obesity: an update. Physiol Rev 2013;93:359–404.
3. Khera AV, Cuchel M, de la Llera-Moya M, et al. Cholesterol efflux capacity, high-density lipoprotein function, and atherosclerosis. N Engl J Med 2011;364:127–35.
4. Lee-Rueckert M, Escola-Gil JC, Kovanen PT. HDL functionality in reverse cholesterol transport–Challenges in translating data emerging from mouse models to human disease. Biochim Biophys Acta 2016;1861:566–83.
5. Tan KC. Reverse cholesterol transport in type 2 diabetes mellitus. Diabetes Obes Metab 2009;11:534–43.
6. Nestel P, Hoang A, Sviridov D, Straznicky N. Cholesterol efflux from macrophages is influenced differentially by plasmas from overweight insulin-sensitive and -resistant subjects. Int J Obes (lond) 2012;36:407–13.
7. Khera AV, Rader DJ. Cholesterol efflux capacity: full steam ahead or a bump in the road? Arterioscler Thromb Vasc Biol 2013;33:1449–51.
8. Low H, Hoang A, Forbes J, et al. Advanced glycation end-products (AGEs) and functionality of reverse cholesterol transport in patients with type 2 diabetes and in mouse models. Diabetologia 2012;55:2513–21.
9. Sabeva NS, Rouse EJ, Graf GA. Defects in the leptin axis reduce abundance of the ABCG5-ABCG8 sterol transporter in liver. J Biol Chem 2007;282:22397–405.
10. Yu L, Hammer RE, Li-Hawkins J, et al. Disruption of Abcg5 and Abcg8 in mice reveals their crucial role in biliary cholesterol secretion. Proc Natl Acad Sci U S A 2002;99:16237–42.
11. Yu L, Li-Hawkins J, Hammer RE, et al. Overexpression of ABCG5 and ABCG8 promotes biliary cholesterol secretion and reduces fractional absorption of dietary cholesterol. J Clin Invest 2002;110:671–80.
12. Langheim S, Yu L, von Bergmann K, et al. ABCG5 and ABCG8 require MDR2 for secretion of cholesterol into bile. J Lipid Res 2005;46:1732–8.
13. Yu L, Gupta S, Xu F, et al. Expression of ABCG5 and ABCG8 is required for regulation of biliary cholesterol secretion. J Biol Chem 2005;280:8742–7.
14. Klett EL, Lu K, Kosters A, et al. A mouse model of sitosterolemia: absence of Abcg8/sterolin-2 results in failure to secrete biliary cholesterol. BMC Med 2004;2:5.
15. Plosch T, Bloks VW, Terasawa Y, et al. Sitosterolemia in ABC-transporter G5-deficient mice is aggravated on activation of the liver-X receptor. Gastroenterology 2004;126:290–300.
16. Yang C, Yu L, Li W, Xu F, Cohen JC, Hobbs HH. Disruption of cholesterol homeostasis by plant sterols. J Clin Invest 2004;114:813–22.
17. Salen G, Shore V, Tint GS, et al. Increased sitosterol absorption, decreased removal, and expanded body pools compensate for reduced cholesterol synthesis in sitosterolemia with xanthomatosis. J Lipid Res 1989;30:1319–30.
18. Lutjohann D, Bjorkhem I, Beil UF, von Bergmann K. Sterol absorption and sterol balance in phytosterolemia evaluated by deuterium-labeled sterols: effect of sitostanol treatment. J Lipid Res 1995;36:1763–73.
19. Yu L, York J, von Bergmann K, Lutjohann D, Cohen JC, Hobbs HH. Stimulation of cholesterol excretion by the liver X receptor agonist requires ATP-binding cassette transporters G5 and G8. J Biol Chem 2003;278:15565–70.
20. Yu XH, Qian K, Jiang N, Zheng XL, Cayabyab FS, Tang CK. ABCG5/ABCG8 in cholesterol excretion and atherosclerosis. Clin Chim Acta 2014;428:82–8.
21. Executive Summary of The Third Report of The National Cholesterol Education Program (NCEP) Expert Panel on Detection, Evaluation, and treatment of high blood cholesterol in Adults (Adult treatment panel III). JAMA 2001;285:2486–97.
22. Lohman T, Roche A, Martorel R. Standardization of anthropometric measurements. Champaign, IL: Human Kinetics Publishers. 1988:39–80.
23. Bonora E, Micciolo R, Ghiatas AA, et al. Is it possible to derive a reliable estimate of human visceral and subcutaneous abdominal adipose tissue from simple anthropometric measurements? Metabolism 1995;44:1617–25.
24. van Haperen R, van Tol A, Vermeulen P, et al. Human plasma phospholipid transfer protein increases the antiatherogenic potential of high density lipoproteins in transgenic mice. Arterioscler Thromb Vasc Biol 2000;20:1082–8.
25. Baila-Rueda L, Cenarro A, Cofan M, et al. Simultaneous determination of oxysterols, phytosterols and cholesterol precursors by high performance liquid chromatography tandem mass spectrometry in human serum. Analytical Methods 2013;5:2249–57.
26. Marzal-Casacuberta A, Blanco-Vaca F, Ishida BY, et al. Functional lecithin:cholesterol acyltransferase deficiency and high density lipoprotein deficiency in transgenic mice overexpressing human apolipoprotein A-II. J Biol Chem 1996;271:6720–8.
27. Jauhiainen M, Metso J, Pahlman R, Blomqvist S, van Tol A, Ehnholm C. Human plasma phospholipid transfer protein causes high density lipoprotein conversion. J Biol Chem 1993;268:4032–6.
28. Julve J, Escola-Gil JC, Ribas V, et al. Mechanisms of HDL deficiency in mice overexpressing human apoA-II. J Lipid Res 2002;43:1734–42.
29. Escola-Gil JC, Lee-Rueckert M, Santos D, Cedo L, Blanco-Vaca F, Julve J. Quantification of in vitro macrophage cholesterol efflux and in vivo macrophage-specific reverse cholesterol transport. Methods Mol Biol 2015;1339:211–33.
30. Bouchard G, Johnson D, Carver T, Paigen B, Carey MC. Cholesterol gallstone formation in overweight mice establishes that obesity per se is not linked directly to cholelithiasis risk. J Lipid Res 2002;43:1105–13.
31. Tran KQ, Graewin SJ, Swartz-Basile DA, Nakeeb A, Svatek CL, Pitt HA. Leptin-resistant obese mice have paradoxically low biliary cholesterol saturation. Surgery 2003;134:372–7.
32. Sabeva NS, Liu J, Graf GA. The ABCG5 ABCG8 sterol transporter and phytosterols: implications for cardiometabolic disease. Curr Opin Endocrinol Diabetes Obes 2009;16:172–7.
33. Wang Y, Su K, Sabeva NS, et al. GRP78 rescues the ABCG5 ABCG8 sterol transporter in db/db mice. Metabolism 2015;64:1435–43.
34. Su K, Sabeva NS, Liu J, et al. The ABCG5 ABCG8 sterol transporter opposes the development of fatty liver disease and loss of glycemic control independently of phytosterol accumulation. J Biol Chem 2012;287:28564–75.
35. Guillemot-Legris O, Mutemberezi V, Cani PD, Muccioli GG. Obesity is associated with changes in oxysterol metabolism and levels in mice liver, hypothalamus, adipose tissue and plasma. Sci Rep 2016;6:10694.

36. Ren S, Ning Y. Sulfation of 25-hydroxycholesterol regulates lipid metabolism, inflammatory responses, and cell proliferation. Am J Physiol Endocrinol Metab 2014;306:E123–30.
37. Naik SU, Wang X, Da Silva JS, et al. Pharmacological activation of liver X receptors promotes reverse cholesterol transport in vivo. Circulation 2006;113:90–7.
38. Escola-Gil JC, Llaverias G, Julve J, Jauhiainen M, Mendez-Gonzalez J, Blanco-Vaca F. The cholesterol content of Western diets plays a major role in the paradoxical increase in high-density lipoprotein cholesterol and upregulates the macrophage reverse cholesterol transport pathway. Arterioscler Thromb Vasc Biol 2011;31:2493–9.
39. Mittendorfer B. Origins of metabolic complications in obesity: adipose tissue and free fatty acid trafficking. Curr Opin Clin Nutr Metab Care 2011;14:535–41.
40. Biddinger SB, Haas JT, Yu BB, et al. Hepatic insulin resistance directly promotes formation of cholesterol gallstones. Nat Med 2008;14:778–82.
41. Grundy SM. Metabolic complications of obesity. Endocrine 2000; 13:155–65.
42. Clement K, Vaisse C, Lahlou N, et al. A mutation in the human leptin receptor gene causes obesity and pituitary dysfunction. Nature 1998;392:398–401.
43. Munzberg H, Bjornholm M, Bates SH, Myers MG Jr. Leptin receptor action and mechanisms of leptin resistance. Cell Mol Life Sci 2005;62:642–52.
44. van der Veen JN, Havinga R, Bloks VW, Groen AK, Kuipers F. Cholesterol feeding strongly reduces hepatic VLDL triglyceride production in mice lacking the liver X receptor alpha. J Lipid Res 2007;48:337–47.
45. Wang HH, Patel SB, Carey MC, Wang DQ. Quantifying anomalous intestinal sterol uptake, lymphatic transport, and biliary secretion in Abcg8(-/-) mice. Hepatology 2007;45:998–1006.
46. Calpe-Berdiel L, Rotllan N, Fievet C, Roig R, Blanco-Vaca F, Escola-Gil JC. Liver X receptor-mediated activation of reverse cholesterol transport from macrophages to feces in vivo requires ABCG5/G8. J Lipid Res 2008;49:1904–11.
47. Dikkers A, de Boer JF, Groen AK, Tietge UJ. Hepatic ABCG5/G8 overexpression substantially increases biliary cholesterol secretion but does not impact in vivo macrophage-to-feces RCT. Atherosclerosis 2015;243:402–6.
48. Bloks VW, Bakker-Van Waarde WM, Verkade HJ, et al. Down-regulation of hepatic and intestinal Abcg5 and Abcg8 expression associated with altered sterol fluxes in rats with streptozotocin-induced diabetes. Diabetologia 2004;47: 104–12.
49. Berge KE, Tian H, Graf GA, et al. Accumulation of dietary cholesterol in sitosterolemia caused by mutations in adjacent ABC transporters. Science 2000;290:1771–5.
50. Lee-Rueckert M, Blanco-Vaca F, Kovanen PT, Escola-Gil JC. The role of the gut in reverse cholesterol transport–focus on the enterocyte. Prog Lipid Res 2013;52:317–28.

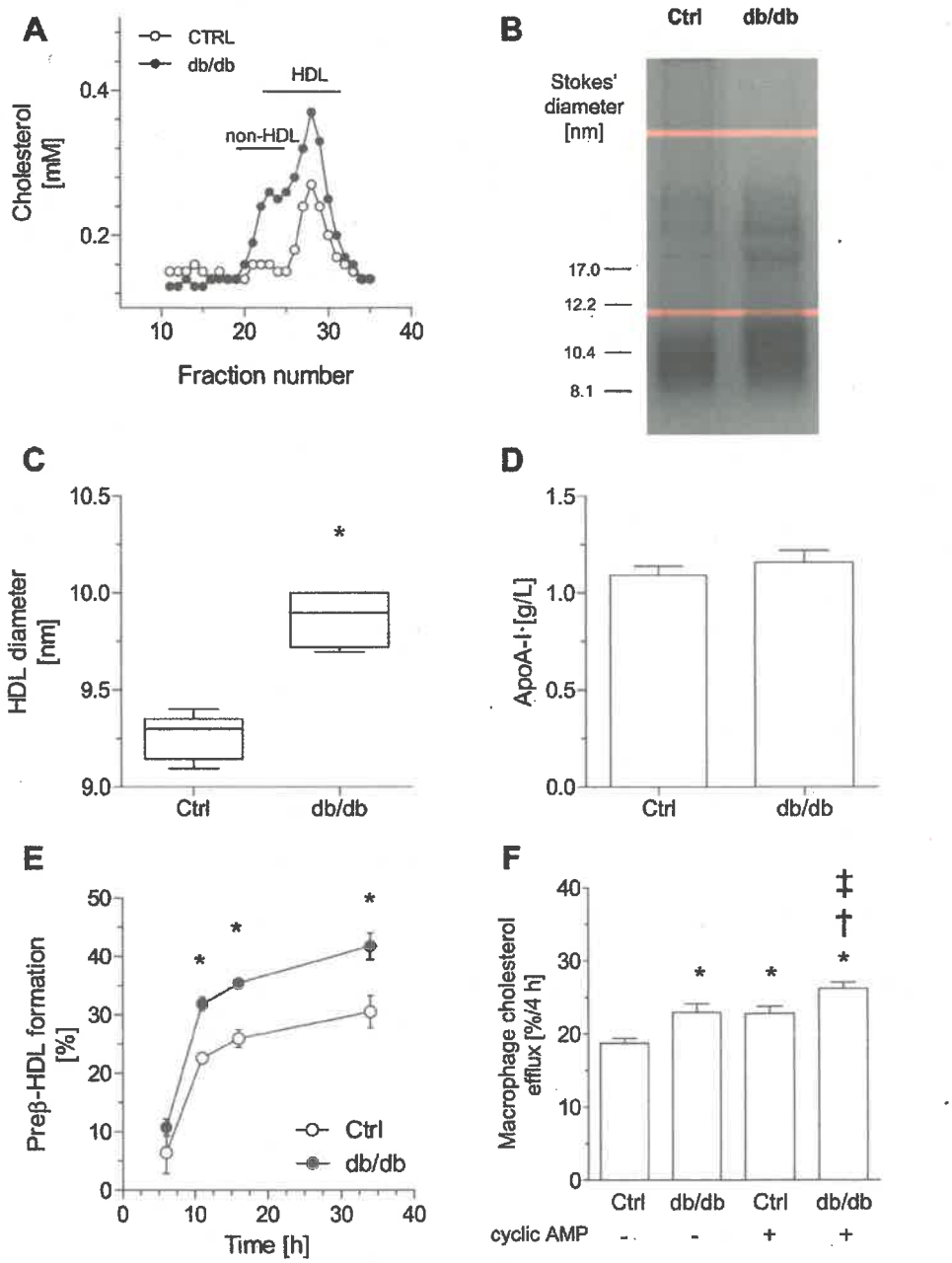

Supplementary Fig 1. High-density lipoprotein (HDL) characterization. **A,** Representative FPLC profile of plasma lipoproteins. Plasma lipoproteins were separated according to their molecular size using 0 Superose 6 columns connected in series in an FPLC system (GE Healthcare). A volume of pooled plasma (3–4 mice/group) was used for lipoprotein fractionation and chromatography and was run under nondenaturing conditions. **B,** Representative image of HDL fractionated by native gradient gel electrophoresis. Plasma samples were prestained with Sudan Black and separated in a 2%–16% gradient gel. **C,** HDL lipoprotein diameters. Lipoprotein diameter was calculated via a molecular weight standard with proteins of known Stokes' diameter (nm; GE Healthcare). Data are expressed as the mean ± SE (n = 4–5 mice/group). **D,** Plasma levels of apoA-I. Data are expressed as the mean ± SE (n = 4 mice/group). ApoA-I was quantified by ELISA with specific polyclonal antibodies against mouse apoA-I. **E,** Formation of preβ-HDL was quantified by two-dimensional crossed immunoelectrophoresis in the presence of an LCAT inhibitor, as described in Materials and Methods. Areas under the curve of percent preβ-HDL formation for each group were calculated. **F,** Macrophage efflux to HDL. Plasma samples were obtained from mice. Next, apoB-containing lipoproteins were removed by phosphotungstic precipitation, and plasma levels of HDL cholesterol were determined enzymatically (n = 10). J774 macrophages were radiolabeled with [^{3}H]-cholesterol (2 μCi/mL). The labeled cells were equilibrated overnight in 0.2% bovine serum albumin (BSA) in the presence/absence of 0.3 mM of cAMP (Sigma-Aldrich) (to upregulate the expression of *Abca1*) and then incubated for 4 hours at 37°C with 5% apoB-containing lipoprotein-depleted plasmas. Percent [^{3}H]-cholesterol efflux to 5.0% phosphotungstic-supernatant was analyzed after 4 hours. Macrophage-specific cholesterol efflux was measured from cells. Data are expressed as the mean ± SE. *$P < 0.05$ compared with control (Ctrl) mice in the absence of cAMP; †$P < 0.05$ compared with db/db mice in the absence of cAMP; or ‡$P < 0.05$ compared with control (Ctrl) mice in the presence of cAMP.

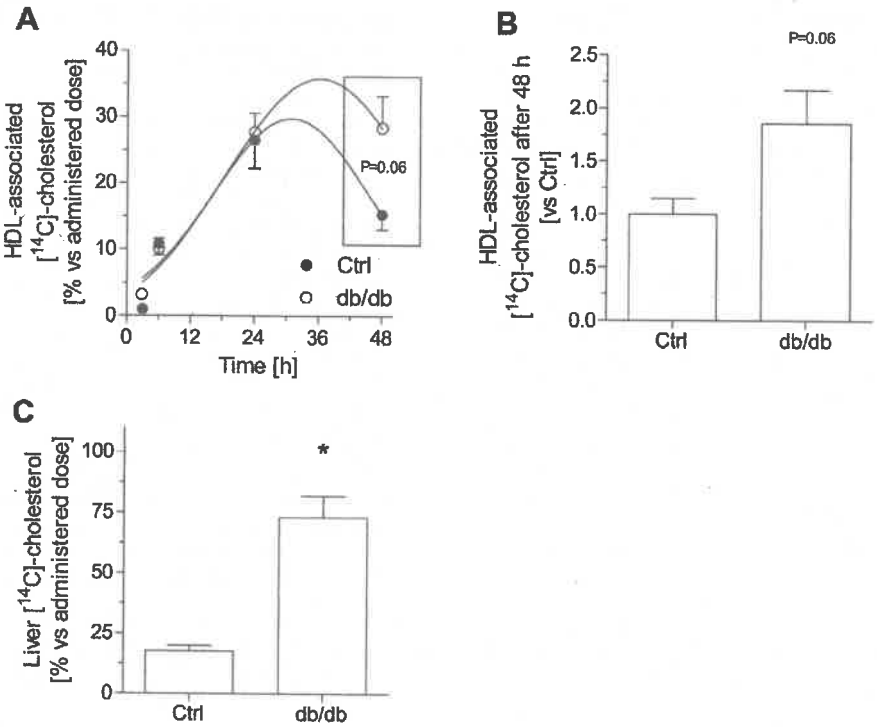

Supplementary Fig 2. Oral fat gavage with [^{14}C]-cholesterol. Serum and liver accumulation of [^{14}C]-cholesterol was measured after a single bolus of 150 μL of radiolabeled olive oil–based emulsion (3 μCi per mouse) over 48 hours. **A**, [^{14}C]-cholesterol was measured in serum at the times indicated. **B**, Area under the curve of HDL-associated [^{14}C]-cholesterol was calculated with data points for 48 h. Data are expressed in relative units vs Ctrl. **C**, [^{14}C]-cholesterol was measured in the liver 48 hours after administration. Results are expressed as the mean ± SE of individual animals (n = 4 mice at each time point). *$P < 0.05$ compared with control (Ctrl) mice. db/db, db/db mice.

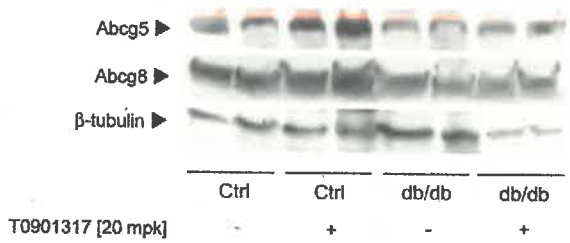

Supplementary Fig 3. Representative immunoblot of hepatic Abcg5/g8 expression. Western blot analysis for mouse Abcg5/g8 was performed on homogenized pieces of liver. Protein extracts underwent 7.5% SDS-polyacrylamide gel electrophoresis under reducing conditions (25 μg of protein per lane) and were then blotted to nitrocellulose membranes. Immunoreactivity was assessed with specific polyclonal antibodies to mouse Abcg5/g8. Mouse β-tubulin was used as a reference protein. Ctrl, control mice; db/db, db/db mice.

Supplementary Table I. Gene expression profile of hepatic markers of lipid metabolism

Genes	Ctrl	db/db	*P*
Apoa1 [vs Ctrl]	1.0 ± 0.2	0.2 ± 0.0	<0.001
Cyp27a1 [vs Ctrl]	1.0 ± 0.2	0.4 ± 0.0	<0.001
Cyp7b1 [vs Ctrl]	1.0 ± 0.3	0.0 ± 0.0	<0.001
Scarb1 [vs Ctrl]	1.0 ± 0.2	0.2 ± 0.0	<0.001
Abcb11 [vs Ctrl]	1.0 ± 0.1	0.1 ± 0.0	<0.001
Pparg [vs Ctrl]	1.0 ± 0.1	1.9 ± 0.1	<0.01
Cd36 [vs Ctrl]	1.0 ± 0.1	5.5 ± 0.5	<0.001
Fasn [vs Ctrl]	1.0 ± 0.2	2.9 ± 0.8	<0.05
Acaca [vs Ctrl]	1.0 ± 0.1	2.0 ± 0.2	<0.01

Abbreviations: Ctrl, control mice; *db/db,* db/db mice.
Data are expressed as mean ± SE (n = 5 mice per group). Differences vs Ctrl were found significant at *P* values lower than 0.05, otherwise is indicated as ns.

Supplementary Table II. Metrics of glucose metabolism

Variables	Ctrl	db/db	*P*
GTT [relative units]*	456 ± 60	1106 ± 416	<0.05
IST [relative units]*	59 ± 12	165 ± 112	<0.05

Abbreviations: Ctrl, control mice; *db/db,* db/db mice; *GTT,* glucose tolerance test; *IST,* insulin sensitivity test.
Data are expressed as mean ± SE (n = 8–12 mice per group). Differences vs Ctrl were found significant at *P* values lower than 0.05.
*Functional tests were all made after a 4-h food deprivation. Blood levels of glucose were monitored either after ip. administration of 1 g/kg of glucose (GTT) or after ip. administration of 0.5 U/kg of porcine insulin, respectively.

Supplementary Table III. Biochemical composition of circulating lipoproteins

Parameters	Ctrl	db/db	*P*
Non-HDL			
Esterified cholesterol [%]	6.5 ± 0.0	16.7 ± 0.4	<0.001
Free cholesterol [%]	4.6 ± 0.0	7.2 ± 0.0	<0.001
Phospholipid [%]	16.2 ± 0.2	27.6 ± 0.5	<0.001
Triglyceride [%]	51.4 ± 1.0	25.6 ± 1.6	<0.001
Protein [%]	21.5 ± 1.0	22.8 ± 1.3	ns
Surface-to-nucleus ratio	0.7 ± 0.0	1.4 ± 0.1	0.1
HDL			
Esterified cholesterol [%]	11.9 ± 0.3	13.5 ± 0.1	<0.01
Free cholesterol [%]	4.2 ± 0.2	3.3 ± 0.1	<0.05
Phospholipid [%]	28.9 ± 0.4	27.5 ± 0.6	ns
Triglyceride [%]	4.9 ± 0.2	4.6 ± 0.2	ns
Protein [%]	50.0 ± 0.3	51.0 ± 0.5	ns
Surface-to-nucleus ratio	5.0 ± 0.1	4.5 ± 0.1	<0.05

Abbreviations: Ctrl, control mice; *db/db,* db/db mice; *HDL,* high-density lipoproteins (density range 1.063 < d < 1.21 g/mL); *non-HDL,* non-HDL fraction (density range 1.006 < d < 1.063 g/mL); *ns,* nonsignificant.
Data are expressed as mean ± SE. Differences vs Ctrl were found significant at *P* values lower than 0.05; otherwise, is indicated as ns. Lipoproteins were isolated by sequential ultracentrifugation from 4–5 independent plasma pools of 2–3 mice each.

Supplementary Table VI. Clinical characteristics and biochemical parameters of the morbidly obese patients (n = 10) undergoing liver biopsy before (baseline) and after (12 mo) weight loss

Parameters	Baseline	12 mo.	P
Anthropometrics			
Weight [kg]	134 ± 7	79 ± 4	<0.001
BMI [kg/m^2]	52 ± 2	31 ± 2	<0.01
Waist [cm]	138 ± 3	96 ± 6	<0.05
Hip [cm]	154 ± 5	128 ± 9	<0.05
TAT [kg]	86 ± 6	33 ± 3	<0.001
Plasma lipids			
Cholesterol [mg/dL]	203 ± 13	163 ± 13	<0.05
LDL-cholesterol [mg/dL]	130 ± 10	99 ± 9	<0.05
HDL-cholesterol [mg/dL]	47 ± 2	46 ± 3	0.8
Liver-related parameters			
ALT [U/L]	35 ± 4	25 ± 3	0.07
GGT [UI/L]	36 ± 7	16 ± 3	<0.01
Triglycerides [mg/g]	90 ± 12	23 ± 5	<0.001
Cholesterol [mg/g]	33 ± 3	3 ± 1	<0.001
Glucose metabolism			
Glucose [mg/dL]	106 ± 6	85 ± 2	<0.01
Insulin [UI/L]	27 ± 5	9 ± 1	<0.01
HOMA-IR*	6 ± 1	1 ± 0	<0.05

Abbreviations: BMI, body mass index; *ALT,* alanine transaminase; *GGT,* γ-glutamyltransferase; *TAT,* total adipose tissue; *HDL,* high-density lipoprotein; *LDL,* low-density lipoprotein.

Results are expressed as the means ± standard deviation (SD; n = 10). Three out of 10 obese subjects included in the study showed T2D (30%).

*HOMA-IR has been calculated excluding patients with T2D. Differences between the mean values before and after surgery (12 mo) were assessed by the nonparametric paired Wilcoxon test or paired t test, as appropriate; differences were considered significant when $P < 0.05$.

Supplementary Table IV. Metrics of HDL catabolism

Variables	HDL_{Ctrl}	$HDL_{db/db}$		P
	Ctrl	Ctrl	db/db	
Fractional catabolic rate [h^{-1}]	0.12 ± 0.01	0.13 ± 0.01	0.07 ± 0.00*	<0.01
Half life [h]	3.16 ± 0.18	3.00 ± 0.47	6.52 ± 1.16*‡	<0.01

Abbreviations: Ctrl, control mice; *db/db,* db/db mice; *HDL_{Ctrl},* HDL isolated from Ctrl mice; *$HDL_{db/db}$,* HDL isolated from db/db mice.
Data are expressed as mean ± SE (n = 4–6 mice per group). Differences between the mean values were assessed by the nonparametric a Kruskal-Wallis followed by Dunn's post-test; differences were considered significant when $P < 0.05$. Specifically, *$P < 0.05$ vs Ctrl group injected with HDL_{Ctrl}; or ‡$P < 0.05$ vs Ctrl group injected with $HDL_{db/db}$.

Supplementary Table V. Effect of LXR agonists on the hepatic levels of radiolabeled cholesterol on an m-RCT setting

Variables	Ctrl	db/db	Ctrl-LXR	db/db-LXR	P
Total activity [% vs injected dose]	1.7 ± 0.4	5.7 ± 0.8*	2.2 ± 0.2	4.7 ± 0.7*‡	0.005
Free cholesterol [% vs injected dose]	1.2 ± 0.3	2.7 ± 0.3*	1.7 ± 0.2	3.1 ± 0.3*‡	0.04

Abbreviations: Ctrl, untreated control mice; *db/db,* untreated db/db mice; *Ctrl-LXR,* LXR agonist-treated Ctrl mice; *db/db-LXR,* LXR agonist-treated db/db mice.
Results are expressed as the mean ± SE (n = 4–7 mice per group). When indicated, mice were treated with the LXR agonist (T0901317) at a dose of 20 mg per kg of body weight during 10 consecutive days. Total activity and free cholesterol represents the relative levels of (^{3}H)-tracer accumulating in the liver 48 h after injection of (^{3}H)-cholesterol-loaded macrophages into mice during the m-RCT assay. The relative levels of free cholesterol were calculated from TLC-fractionated lipid extracts. Differences between mean values were assessed by the nonparametric Kruskal-Wallis test followed by Dunn's post-test or ANOVA followed a Newman-Keuls post-test, as appropriate; differences were considered significant when $P < 0.05$. Specifically, *$P < 0.05$ vs Ctrl group; or ‡$P < 0.05$ vs LXR agonist-treated Ctrl mice.